1973

Analysis of a superconducting generator for ship propulsion.

Denizmen, Kustal A.

Massachusetts Institute of Technology

ANALYSIS OF A SUPERCONDUCTING GENERATOR FOR SHIP PROPULSION.

Kutsal A. Denizmen

ANALYSIS OF A SUPERCONDUCTING GENERATOR FOR SHIP PROPULSION

by

KUTSAL A. DENIZMEN
LTJG, Turkish Navy

B.S., Turkish Naval Academy
(1968)

SUBMITTED IN PARTIAL FULFILLMENT OF THE REQUIREMENTS FOR THE DEGREE OF MASTER OF SCIENCE IN MECHANICAL ENGINEERING AND THE PROFESSIONAL DEGREE OF OCEAN ENGINEER

at the

MASSACHUSETTS INSTITUTE OF TECHNOLOGY
May, 1973

Analysis of a Superconducting Generator for Ship Propulsion

Kutsal A. Denizmen

Abstract

Application of superconducting electrical machinery to ship propulsion yields light weight and small volume propulsion plants with increased system efficiency, reliability and lower cost. Such propulsion systems might be the only feasible answer for high performance ship types.

A design method for two-pole synchronous machine with superconducting field winding is developed which will survive even under the worse fault conditions. Iron shielded machines with the effects of higher harmonics and partial winding angles are considered. The method is then adapted to a computer program for ease of obtaining minimum volume and weight machines. The results are compared with 20,000 HP conventional propulsion generator. It is shown that great weight and volume savings are possible.

Thesis Supervisor: J.L. Smith, Jr.
Title: Professor of Mechanical Engineering

ACKNOWLEDGEMENTS

The author wishes to thank Professor J.L. Smith, Jr. for his support and encouragement during the preparation of this thesis. The author is also in debt to Dr. T.A. Keim, for his explanations and answers to so many questions which made this thesis possible. Special thanks to Professor J.L. Kirtley, Jr. and Professor P. Thullen, for making themselves available for discussions. The author would also like to thank Professor W. Dietz for his suggestions.

The author is grateful to his wife, Nilgün, for her patience and understanding during the years he spent at MIT. Finally, special thanks to Mrs. Pilar Zuniga who did a beautiful piece of work when typing this thesis.

TABLE OF CONTENTS

LIST OF TABLES

LIST OF FIGURES

NOMENCLATURE

Subscripts

a	armature winding
f	field winding
r	radial
θ	azimuthal
i	inside (for field quantities--at a radius less than inner radius)
i	inner (when used with a dimension)
o	outside (when used with a field quantity)
o	outer (when used with a dimension)
s	field quantities, generated by a sheet current
a	phase a
b	phase b
c	phase c
d	direct axis-armature
q	quadrature axis-armature
sd	direct axis-damper shield
sq	quadrature axis-damper shield

Symbols

B	magnetic flux density
B_{sat}	saturation flux density of shield material
B_{av}^2	mean-squared field experienced by armature conductors
d_w	diameter of primary conductor
d_{sh}	dissipation density of shield material (watts/lb)

E_f	open circuit voltage (RMS)
E_f''	voltage behind subtransient reactance
e_f''	voltage behind subtransient reactance (per unit)
H	magnetic field density
i	current
I_a	rated armature current (RMS)
J	current density
J_a	rated armature-current density
J_f	rated field-current density
h	shield structure thickness
h_h	primary shield thickness
ℓ	straight-section length
ℓ_t	total machine length
ℓ_a	effective length for calculating armature self inductance
ℓ_f	effective length for calculating field-winding self-inductance
ℓ_m	effective length for calculating field-to-armature mutual inductance
ℓ_d	effective length for calculating damper self-inductance
ℓ_{ad}	effective length for calculating damper-to-armature mutual inductance
ℓ_{fd}	effective length for calculating field-to-damper mutual inductance
ℓ_c	length of armature conductors
ℓ_{ed}	effective length for calculating eddy-current losses
ℓ_{sh}	effective length for calculating shield losses
L_a	self inductance, armature phase

L_f self inductance, field

L_{ab} mutual inductance, phase-to-phase

L_{ad} mutual inductance, armature-to-damper

L_{fd} mutual inductance, field-to-damper

M magnitude of mutual inductance, field-to-armature

M_a mutual inductance, field-to-phase-a

M_s magnitude of mutual inductance, damper-to-phase-a

N_{at} number of turns in armature winding

N_{ft} number of turns in field winding

p number of pole pairs

P rated volt-amperes

P_c conduction losses

P_{ed} eddy-current losses

P_{sh} shield dissipation

R_s inner radius, shield

R_{os} outer radius, shield

R_t outer radius, damper shield

V_t rated terminal voltage

X_a synchronous impedance (in ohms)

x_a per-unit synchronous impedance, normalized to internal voltage, E_f

X_d per-unit synchronous impedance, with V_t as base voltage

X_d' per-unit transient reactance (direct axis)

X_d'' per-unit subrtansient reactance

$x = R_{ai}/R_{ao}$

$y = R_{fi}/R_{fo}$

δ skin depth

θ angular displacement

θ_{wf} field-winding included angle

$\theta_{wfe} = p\theta_{wf}$

θ_{wa} armature winding angle

$\theta_{wae} = p\theta_{wa}$

σ_o magnitude of maximum radial stress under three phase fault from load

σ_r radial stresses

τ sheer stresses

ρ density

σ conductivity of armature conductors

σ_t conductivity of damper-shield material

ϕ rotor-axis displacement from axis of phase-a

ω angular frequency, also used for deflections

ω_e electrical angular frequency = $p\omega$

INTRODUCTION

Advantages of electrical ship propulsion systems were realized years ago. Some of them are: arrangement flexibility, ease of automation and possible integration to ship service power. Major drawbacks were the relatively high cost and weight of system components.

Over the past ten years or so many studies have been done on the possible applications of superconductors to electrical power equipment, with most effort devoted to transformers with decreasing attention given to transmission, ac machines, and dc machines respectively. The development of high-field superconducting wire, suitable for fabrication into windings for electric machines, high vacuum seals and rotating dewar technology, made applications of superconductors possible for rotating electric machines.

Among the many different types of superconductors,the most useful one is type II, because of its ability to carry a high current density in a high magnetic field, and the first major consequence of this upon machine design is that we may break free from the magnetic limitations of iron. Elimination of iron will reduce the machine weight and provide more armature conductors for a given space, thus increasing the power rating per unit volume. If the flux density at the armature conductors is increased by a factor of 3 over that in a conventional machine, the generated emf per unit length of conductor is thus increased 3 times, if the armature diameter and the rotor speed are left unchanged. Therefore, for the same output power and current, the machine length can be reduced by the factor 3, with a corresponding reduction in machine volume and weight.

Application of superconductors to rotating machines is not without problems. First of all, they will operate only at extremely low temperatures. Secondly, perhaps the most important one is that time varying magnetic fields produce

losses which are prohibitive at power frequencies. These losses are the limiting factor for the application of superconductors to field windings. Therefore, the configuration of a superconducting machine must be a superconducting stationary or rotating field winding and a normally conducting ac armature winding, which may also be rotating or stationary. Configuration for rotating armature has inherent problem of transmitting power across sliding contacts. With the advent of rotatable liquid helium transfer coupling[1], a rotating superconducting field winding became practical, thus eliminating the necesity for rotating the armature. Different designs and configurations have been studied in different countries, among them synchronous machines[5,6,7], dc machines[3], homopolar machines[3,4], double armature machines[1]. and the toroidal reciprocating alternator[2]. Some of them are already built or under development.

Application of superconducting electric machinery to ship propulsion systems has been studied over approximately the past seven years[7,8,9,10,11]. A superconducting propulsion system is shown in Figure 1. The required set of performance characteristics from a propulsion plant will depend mainly on the ship type being considered. Such characteristics are tied with the options, control and type of electric machinery. For example, bulk carriers which run at their full speed 85% of their operating time will not require speed control as much as a naval combatant vessel, and the option box may be omitted and a simple synchronous-synchronous drive in which the propeller speed can be controlled by varying prime mover speed, may be used. Destroyers, which operate over their full speed range, will require more sophisticated controls and the option box may be filled with a cyloconverter if a synchronous system is used or dc machinery might be more appropriate. It should be pointed out that the choice of thruster and prime mover will also affect the electric machinery.

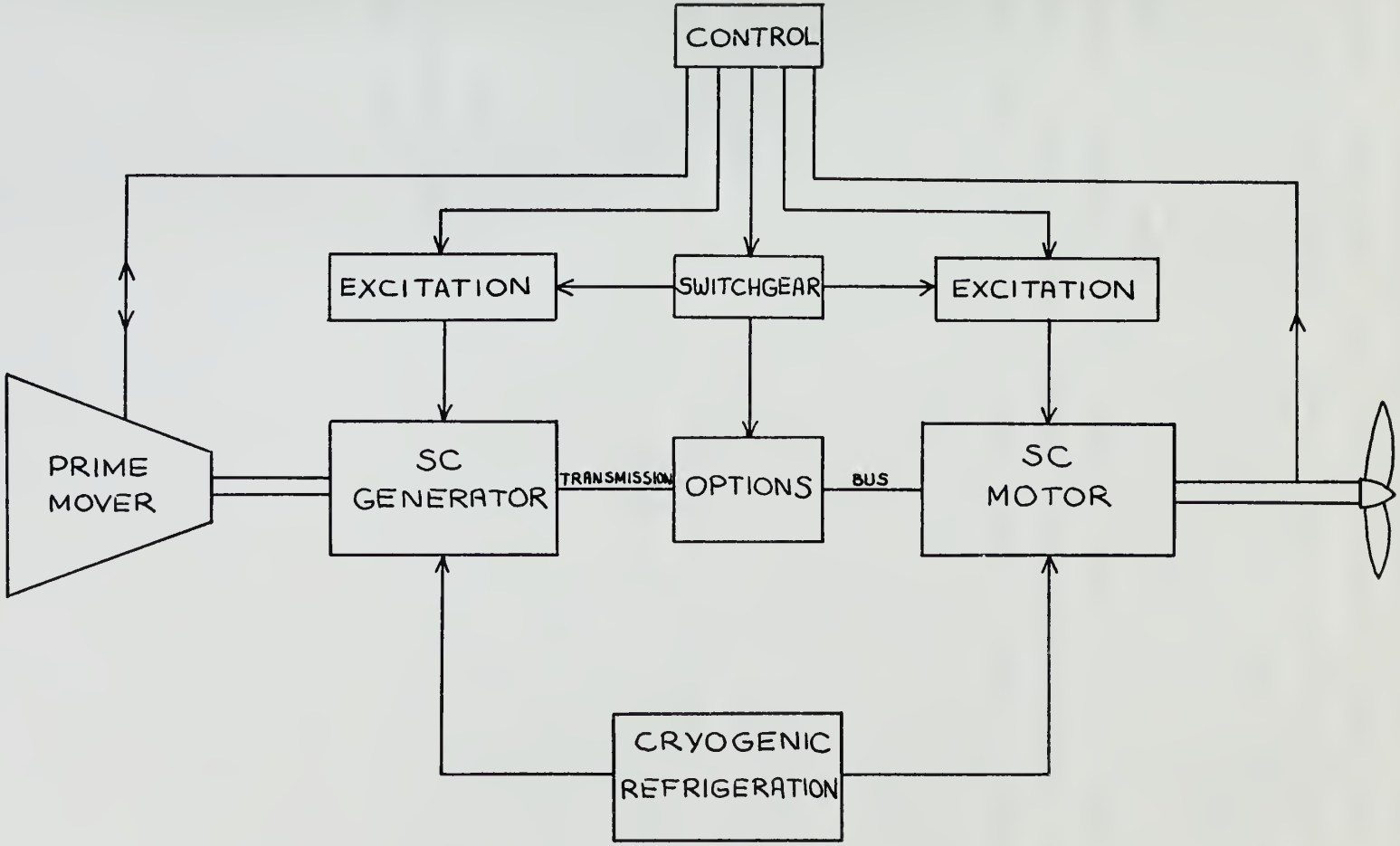

Figure 1
Superconducting Electric Propulsion System

Recently some studies have been done on conventional electric propulsion of bulk carriers[12,13,14]. Sixteen tankers, container ships and LNG carriers are being built or are under design. Conventional electric propulsion systems have been selected due to the fact that flexibility of propulsion systems may lead to possible savings in the volume of the plant. Gas turbine generator sets can be placed on the main deck, reducing the inlet and exhaust ducting volume and flow pressure drops, thus improving gas turbine performance. Added to these advantages, if a superconducting drive is used even more savings are possible. It can be shown that[15] the reduction of specific machinery weight from 30 to 10 lbs/SHP will permit an increase in maximum speed from 35 to 50 knots with no sacrifice in payload or endurance for a destroyer type ship. Introduction of gas turbines has made specific weights somewhat lower, but introduced new problem areas. Newly developed ship types such as hydrofoils, SES and catamarans which require unusual propulsion plant arrangements, suffer greatly with conventional propulsion plants. With increased power levels required by high performance ship types, superconducting electric propulsion plants may be the only feasible answer. The purpose of this thesis is to obtain a design method for synchronous machines which can be used to realize possible advantages.

Chapter 1
DEVELOPMENT OF A MODEL

1A Model Configuration

The geometrical model used for this analysis is illustrated in Figure 2 and Figure 3, with approximate account taken of the effects of end turns as indicated by measurements made on the first MIT experimental machine[5]. The axial length of one set of armature end turns is taken to be equal to the average armature winding diameter in the active section divided by the number of pole pairs, and the radial thickness of the end turns is assumed equal to twice the radial thickness of the armature winding in the active region. These relatively large end turns are assumed because there is more copper in the active region and more volume is needed in which to cross the phase conductors over each other.

The machine has a smooth outer shell made of either laminated iron or a highly conducting material, such as copper or aluminum, in order to provide a uniform boundary condition and confine the magnetic field within the machine. In the case of conductive image shield, circulating image currents serve to confine the magnetic field.

There is a thin highly conductive shield between the field winding and armature which rotates with the field winding. The purpose of this shell is to intercept asynchronous magnetic fields due to load imbalance and space harmonics of the armature field and take large fault torques and radial loads under fault conditions[1,18]. It may also intercept thermal radiation from the room temperature armature or a separate thermal radiation shield may be used. In any case, the essential purpose of this shell is to protect the field windings. Since this shell will not be strong enough to take large fault loadings, it should possibly be supported by a shell made out of a stronger material. In this work, the load carrying structure will

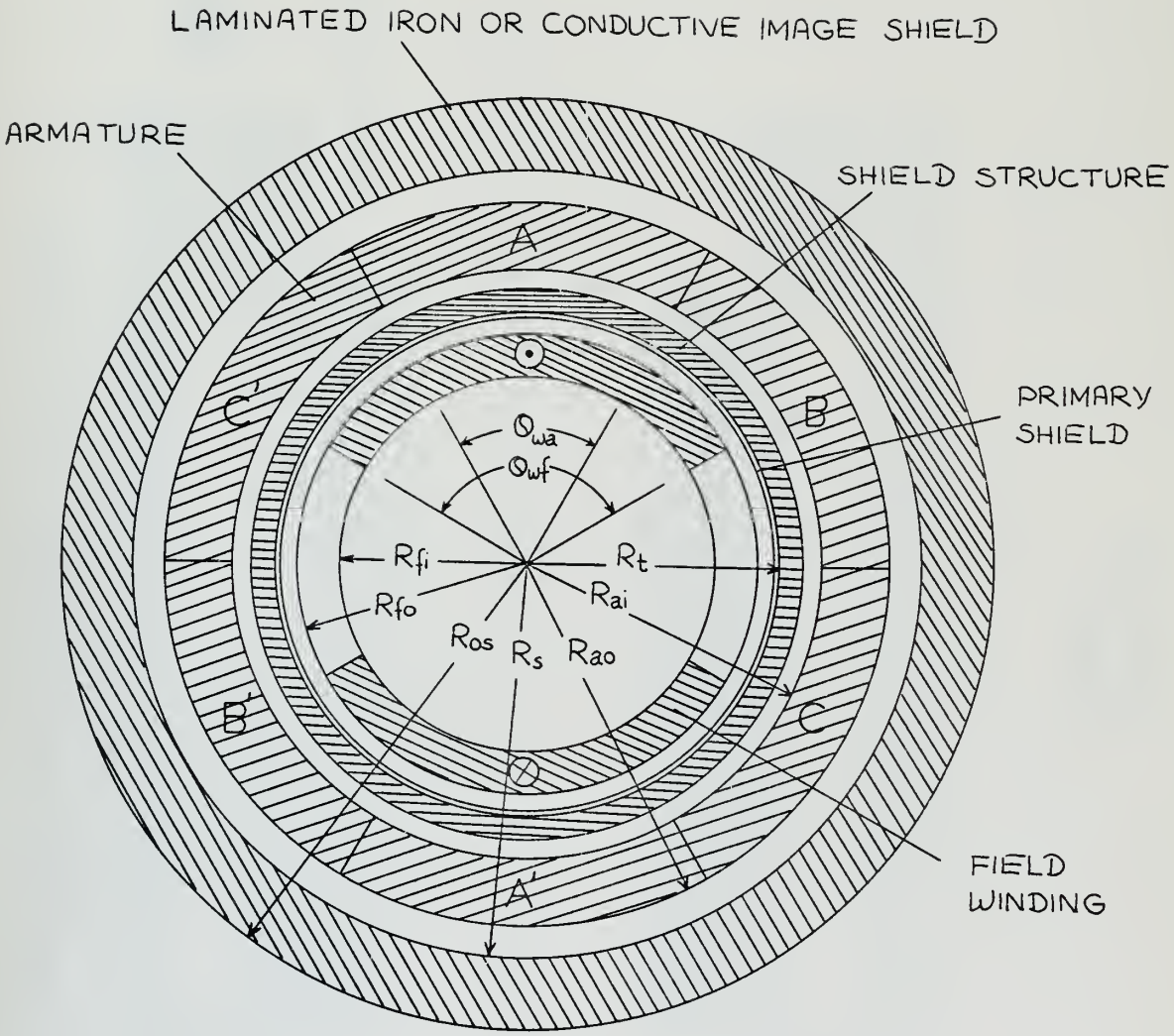

Figure 2
Cross Sectional View

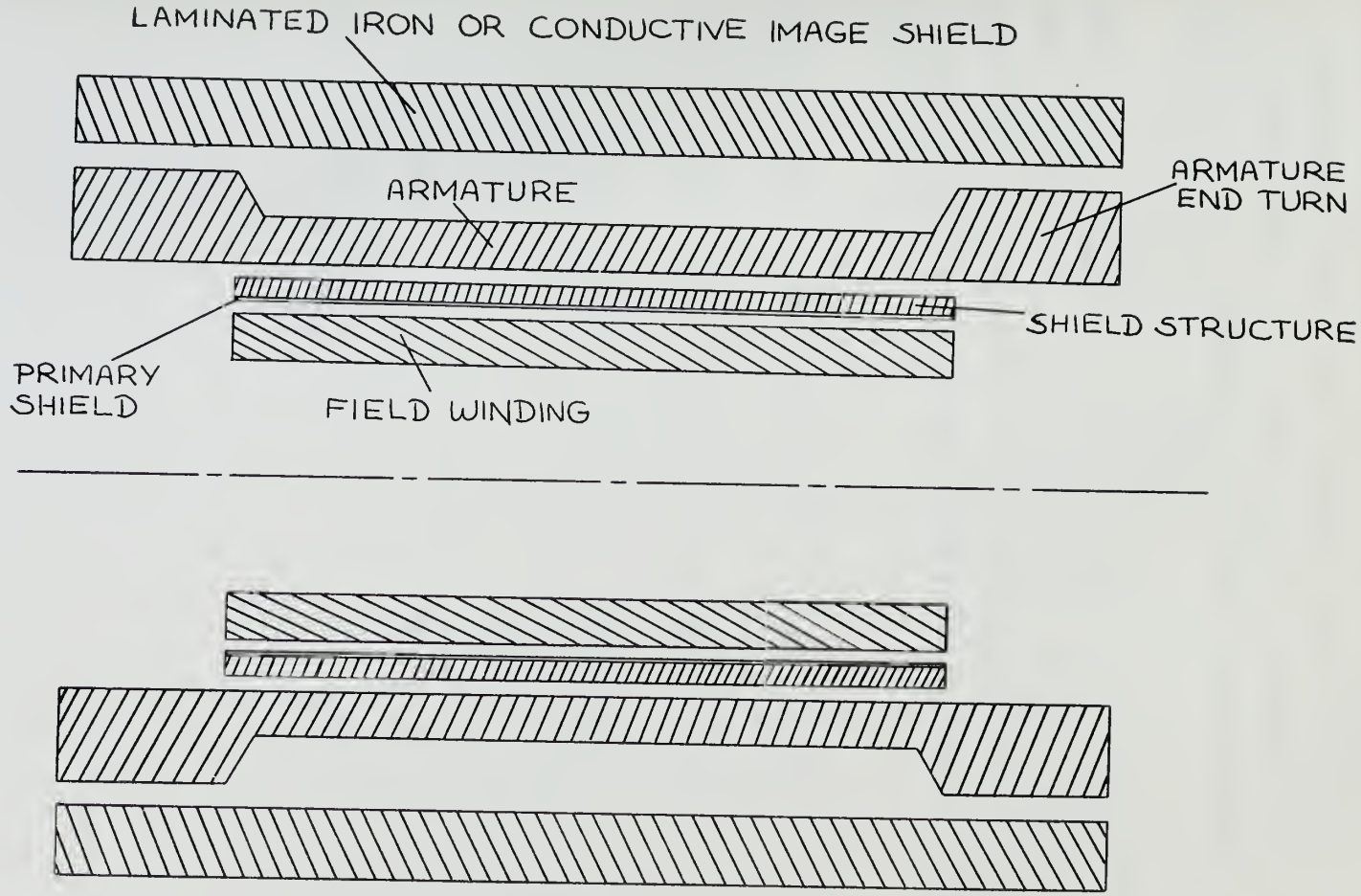

Figure 3
Side View

be called the shield structure and the shell which provides actual shielding will be called the primary shield. Shown in Figures 2 and 3, the primary shield is inside the shield structure, but it may very well be outside the shield structure. Consequences of these configurations will be discussed in a later section.

The electrical configuration is shown in Figure 4. There are a total of six windings, three phase, one field and a direct and a quadrature axis damper winding. The electrical parameters of the machine are the coefficients of the flux-current relationship which can be expressed in matrix form[16,17]:

$$\begin{pmatrix} \lambda_a \\ \lambda_b \\ \lambda_c \\ \lambda_f \\ \lambda_{sd} \\ \lambda_{sq} \end{pmatrix} = \begin{pmatrix} L_a & L_{ab} & L_{ab} & M_a & L_{ad} & L_{aq} \\ L_{ab} & L_a & L_{ab} & M_b & L_{bd} & L_{bq} \\ L_{ab} & L_{ab} & L_a & M_c & L_{cd} & L_{cq} \\ M_a & M_b & M_c & L_f & L_{fd} & 0 \\ L_{ad} & L_{bd} & L_{cd} & L_{fd} & L_d & 0 \\ L_{aq} & L_{bq} & L_{cq} & 0 & 0 & L_d \end{pmatrix} \begin{pmatrix} i_a \\ i_b \\ i_c \\ i_f \\ i_d \\ i_q \end{pmatrix}$$

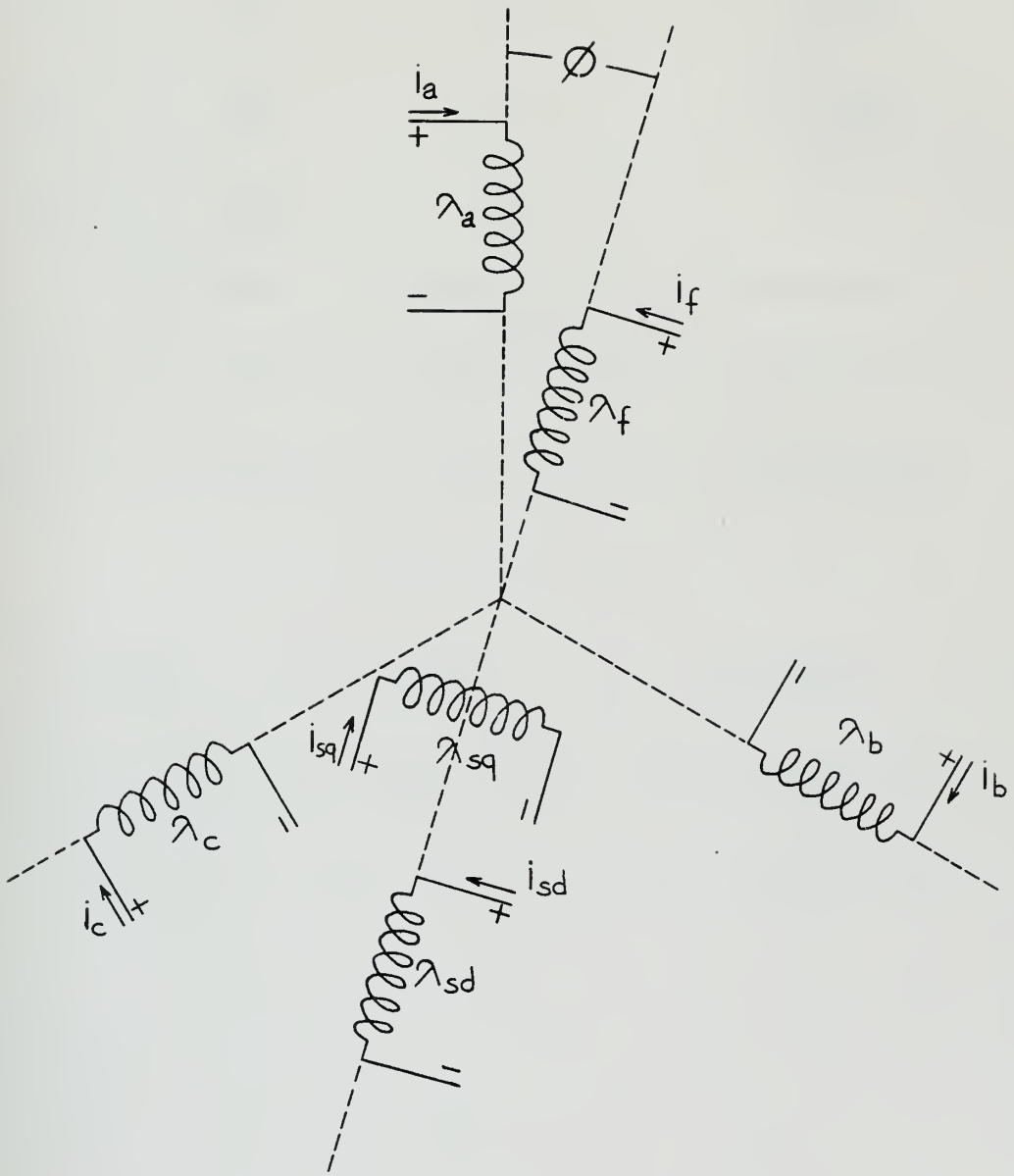

Figure 4
Electrical Configuration

This may be expressed by:

$$\begin{bmatrix} \lambda_a \\ \lambda_b \\ \lambda_c \\ \lambda_f \\ \lambda_{sd} \\ \lambda_{sq} \end{bmatrix} = \begin{bmatrix} L_a & L_{ab} & L_{ab} \\ L_{ab} & L_a & L_{ab} \\ L_{ab} & L_{ab} & L_a \\ M\cos p\phi & M\cos p(\phi-2\pi/3) & M\cos p(\phi+2\pi/3) \\ M_s\cos p\phi & M_s\cos p(\phi-2\pi/3) & M_s\cos p(\phi+2\pi/3) \\ M_s\sin p\phi & M_s\sin p(\phi-2\pi/3) & M_s\sin p(\phi+2\pi/3) \end{bmatrix}$$

$$\begin{bmatrix} M\cos p\phi & M_s\cos p\phi & M_s\sin p\phi \\ M\cos p(\phi-2\pi/3) & M_s\cos p(\phi-2\pi/3) & M_s\sin p(\phi-2\pi/3) \\ M\cos p(\phi+2\pi/3) & M_s\cos p(\phi+2\pi/3) & M_s\sin p(\phi+2\pi/3) \\ L_f & L_{fd} & 0 \\ L_{fd} & L_d & 0 \\ 0 & 0 & L_d \end{bmatrix} \begin{bmatrix} i_a \\ i_b \\ i_c \\ i_f \\ i_{sd} \\ i_{sq} \end{bmatrix}$$

By doing so, it is assumed that all rotor-to-armature mutual inductances vary sinusoidally with rotor position. This is equivalent to neglecting higher order harmonics. It should be emphasized that higher order harmonics in phase-to-phase mutual inductances were not neglected in this study.

1B Field Analysis

For the purposes of this study, a two dimensional representation is used. The effects of finite length and end turn geometry will be included in an approximate fashion. In the straight, active section of the machine, currents are parallel to the axis of the machine and effective armature and field current densities are related to terminal current by

$$J_a = \frac{2\, I_a\, N_{at}}{\theta_{wae}\, R_{ao}^{\,2}(1-x^2)} \qquad (1)$$

$$J_f = \frac{2\, I_f\, N_{ft}}{\theta_{wfe}\, R_{fo}^{\,2}(1-y^2)} \qquad (2)$$

The field and armature winding are assumed to have a uniform density between their inner and outer radii, and to fill the wedged shape space within a winding angle. Expressions for the magnetic fields generated by these currents are derived in references 16 and 17, and are summarized in Table 1. Wherever double signs ($\pm$ or $\mp$) appear, the upper sign refers to the laminated iron shield case, the lower to the conductive image shield case. Unless otherwise specified, all current densities take space factors into account.

TABLE 1

MAGNETIC FIELDS

Field Winding Fields

$r<R_{fi}$

$np\neq 2$

$$H_{rf}= -\sum_{n\ odd} \frac{2J_f \sin\left(\frac{n\theta_{wfe}}{2}\right)\sin np(\theta-\phi)}{n\pi(2-np)} r\left(\frac{r}{R_{fo}}\right)^{np-2} \quad x$$

$$\left[1-y^{2-np}\pm\left(\frac{2-np}{2+np}\right)\left(\frac{R_{fo}}{R_s}\right)^{2np}(1-y^{2+np})\right]$$

if p=2, n=1 component:

$$-\frac{J_f \sin\left(\frac{\theta_{wfe}}{2}\right)\sin 2(\theta-\phi)}{\pi} r\left[-\ln y\pm\tfrac{1}{4}(1-y^4)\left(\frac{R_{fo}}{R_s}\right)^4\right]$$

$np\neq 2$

$$H_{\theta f}= -\sum_{n\ odd} \frac{2J_f \sin\left(\frac{n\theta_{wfe}}{2}\right)\cos np(\theta-\phi)}{n\pi(2-np)} r\left(\frac{r}{R_{fo}}\right)^{np-2} \quad x$$

$$\left[1-y^{2-np}\pm\left(\frac{2-np}{2+np}\right)\left(\frac{R_{fo}}{R_s}\right)^{2np}(1-y^{2+np})\right]$$

if p=2, n=1 component:

$$-\frac{J_f \sin\left(\frac{\theta_{wfe}}{2}\right)\cos 2(\theta-\phi)}{\pi} r\left[-\ln y\pm\tfrac{1}{4}(1-y^4)\left(\frac{R_{fo}}{R_s}\right)^4\right]$$

Table 1
Magnetic Fields (continued)

$R_{fi}<r<R_{fo}$

$np\neq 2$

$$H_{rf}= -\sum_{n\ odd} \frac{2J_f \sin\left(\frac{n\theta_{wfe}}{2}\right)\sin np(\theta-\phi)}{n\pi(4-n^2p^2)} r\left[-2np-(2-np)\left(\frac{R_{fi}}{r}\right)^{np+2}\right.$$

$$\left.+(2+np)\left(\frac{r}{R_{fo}}\right)^{np-2} \pm(2-np)\left(\frac{r}{R_s}\right)^{np-2}\left(\frac{R_{fo}}{R_s}\right)^{np+2}(1-y^{np+2})\right]$$

if p=2, n=1 component:

$$-\frac{J_f \sin\left(\frac{\theta_{wfe}}{2}\right)\sin 2(\theta-\phi)}{4\pi} r\left[1-\left(\frac{R_{fi}}{r}\right)^4+4\ln\left(\frac{R_{fo}}{r}\right)\pm\left(\frac{R_{fo}}{R_s}\right)^4(1-y^4)\right]$$

$np\neq 2$

$$H_{\theta f}= -\sum_{n\ odd} \frac{2J_f \sin\left(\frac{n\theta_{wfe}}{2}\right)\cos np(\theta-\phi)}{n\pi(4-n^2p^2)} r\left[-4+(2-np)\left(\frac{R_{fi}}{r}\right)^{np+2}\right.$$

$$\left.+(2+np)\left(\frac{r}{R_{fo}}\right)^{np-2} \pm(2-np)\left(\frac{r}{R_s}\right)^{np-2}\left(\frac{R_{fo}}{R_s}\right)^{np+2}(1-y^{np+2})\right]$$

if p=2, n=1 component:

$$-\frac{J_f \sin\left(\frac{\theta_{wfe}}{2}\right)\cos 2(\theta-\phi)}{4\pi} r\left[-1+\left(\frac{R_{fi}}{r}\right)^4+4\ln\left(\frac{R_{fo}}{r}\right)\right.$$

$$\left.\pm\left(\frac{R_{fo}}{R_s}\right)^4(1-y^4)\right]$$

Table 1
Magnetic Fields (continued)

R_{fo} r R_s

$$H_{rf} = -\sum_{n\ odd} \frac{2J_f \sin\left[\frac{n\theta_{wfe}}{2}\right] \sin np(\theta-\phi)}{n\pi(2+np)} r\left[\frac{R_{fo}}{r}\right]^{np+2} (1-y^{np+2}) \quad x$$

$$\left[1 \pm \left(\frac{r}{R_s}\right)^{2np}\right]$$

$$H_{\theta f} = -\sum_{n\ odd} \frac{2J_f \sin\left[\frac{n\theta_{wfe}}{2}\right] \cos np(\theta-\phi)}{n\pi(2+np)} r\left[\frac{R_{fo}}{r}\right]^{np+2} (1-y^{np+2}) \quad x$$

$$\left[1 \mp \left(\frac{r}{R_s}\right)^{2np}\right]$$

To get Armature phase A fields

Replace	By
$\theta-\phi$	θ
J_f	J_a
y	x
θ_{wfe}	θ_{wae}
R_{fi}	R_{ai}
R_{fo}	R_{ao}

1C Inductance Parameters

Self and mutual inductances of and between the various windings are calculated by integrating flux linkage of the fields given in Table 1, over the area of a winding. Reference 16 gives such a calculation and the results taken from this reference are summarized in Table 2.

The electrothermal shield has been treated as a fourier series of sinusoidally wound damper windings. The justification for this is that each space harmonic field will excite currents in this shell that are sinusoidally distributed in angle. Further more, each space harmonic is orthogonal to all but one of the ficticious windings. Each winding is characterized by a self inductance and mutual inductances with field and armature windings. The mutual inductance between any two of these damper windings is zero. Included in the expressions, Nnp is fictitious number of turns of damper winding.

The expressions given in Table 2 have been left with the effective length noted differently for each parameter. These lengths may not correspond to any physical lengths of machine parts, because of the effects of end turns. Further more, since end turns of different coils in a machine will have different lengths, we may expect the coils to have differing effective lengths. Certain assumptions utilized when evaluating effective lengths are discussed in section D of this chapter.

TABLE 2

INDUCTANCES

$np \neq 2$

$$L_f = \sum_{n\ \text{odd}} \frac{16\, \ell_f \mu_o\, N_{ft}^2 \sin^2\left[\frac{n\theta_{wfe}}{2}\right]}{n^3 p \pi \theta_{wfe}^2 (n^2p^2-4)(1-y^2)^2}\left[(np-2)+4y^{np+2}\right.$$

$$\left.-(np+2)y^4 \pm 2\left[\frac{np-2}{np+2}\right](1-y^{np+2})^2\left[\frac{R_{fo}}{R_s}\right]^{2np}\right]$$

if p=2, n=1 component:

$$\frac{8\, \ell_f \mu_o\, N_{ft}^2 \sin^2\left[\frac{\theta_{wfe}}{2}\right]}{\pi \theta_{wfe}^2 (1-y^2)^2}\left(y^4 \ln y + \frac{1-y^4}{4} \pm \frac{(1-y^4)^2}{8}\left[\frac{R_{fo}}{R_s}\right]^4\right)$$

$np \neq 2$

$$L_a = \sum_{n\ \text{odd}} \frac{16\, \ell_a\, \mu_o\, N_{at}^2 \sin^2\left[\frac{n\theta_{wae}}{2}\right]}{n^3 p \pi \theta_{wae}^2 (n^2p^2-4)(1-x^2)^2}\left[(np-2)+4x^{np+2}\right.$$

$$\left.-(np+2)x^4 \pm 2\left[\frac{np-2}{np+2}\right](1-x^{np+2})^2\left[\frac{R_{ao}}{R_s}\right]^{2np}\right]$$

if p=2, n=1 component:

$$\frac{8\, \ell_a\, \mu_o\, N_{at}^2 \sin^2\left[\frac{\theta_{wae}}{2}\right]}{\pi \theta_{wae}^2 (1-x^2)^2}\left(x^4 \ln x + \frac{1-x^4}{4} \pm \frac{(1-x^4)^2}{8}\left[\frac{R_{ao}}{R_s}\right]^4\right)$$

$$M = \sum_{n\ odd} M_n \cos np\phi$$

where

$$M_n = \frac{32\ \ell_m \mu_o\ N_{at}\ N_{ft}\ \sin\left[\frac{n\theta_{wae}}{2}\right] \sin\left[\frac{n\theta_{wfe}}{2}\right] (1-y^{np+2})}{n^2\pi\ \theta_{wae}\ \theta_{wfe}(1-y^2)(1-x^2)} \left[\frac{R_{fo}}{R_{ao}}\right]^{np} Cnp$$

and

$$C_{np} = \frac{\left[1-x^{2-np} \pm \left[\frac{2-np}{2+np}\right](1-x^{2+np}) \left[\frac{R_{ao}}{R_s}\right]^{2np}\right]}{np[4-(np)^2]} \qquad \text{for } np \neq 2$$

if p=2, n=1 component:

$$C_2 = \left[-\frac{1}{4} \ln x \pm \frac{1-x^4}{16} \left[\frac{R_{ao}}{R_s}\right]^4\right]$$

$$L_{dn} = \frac{\mu_o \ell_d\ \pi\ N_{np}^2}{8np}\left[1 \pm \left[\frac{R_t}{R_s}\right]^{2np}\right]$$

$np \neq 2$

$$L_{adn} = \frac{2\mu_o \ell_{ad}\ N_{at}\ N_{np}\ \sin\left[\frac{n\theta_{wae}}{2}\right] \cos np\phi}{n^2 p\ \theta_{wae}(1-x^2)(2-np)} \left[\frac{R_t}{R_{ao}}\right]^{np} \left[1-x^{2-np} \pm \left[\frac{2-np}{2+np}\right] X\right.$$

$$\left.(1-x^{2+np}) \left[\frac{R_{ao}}{R_s}\right]^{2np}\right]$$

if p=2, n=1 component:

$$L_{adl} = \frac{\mu_o \ell_{ad}\ N_{at}\ N_{np}\ \sin\left[\frac{\theta_{wae}}{2}\right] \cos 2\phi}{\theta_{wae}(1-x^2)} \left[-\ln x \pm \frac{1-x^4}{4} \left[\frac{R_{ao}}{R_s}\right]^4\right] \left[\frac{R_t}{R_{ao}}\right]^2$$

$np \neq 2$

$$L_{ab} = \sum_{n \text{ odd}} \frac{16\, \ell_a \mu_o N_{at}^2 \sin^2\left[\frac{n\theta_{wae}}{2}\right] \cos\left[\frac{2n\pi}{3}\right]}{n^3 p \pi \theta_{wae}^2 (n^2p^2-4)(1-x^2)^2} \left[(np-2)+4x^{np+2}\right.$$

$$\left. -(np+2)x^4 \pm 2\left[\frac{np-2}{np+2}\right](1-x^{np+2})^2\left[\frac{R_{ao}}{R_s}\right]^{2np}\right]$$

If $p=2$, $n=1$ component:

$$-\frac{4\, \ell_a \mu_o N_{at}^2 \sin^2\left[\frac{\theta_{wae}}{2}\right]}{\pi \theta_{wae}^2 (1-x^2)^2}\left(x^4 \ln x + \frac{1-x^4}{4} \pm \frac{(1-x^4)^2}{8}\left[\frac{R_{ao}}{R_s}\right]^4\right)$$

$$L_a - L_{ab} = \frac{16\, \ell_a \mu_o N_{at}^2}{\pi \theta_{wae}^2 (1-x^2)^2} \sum_{n \text{ odd}} \frac{\sin^2\left[\frac{n\theta_{wae}}{2}\right]\left(1-\cos\left[\frac{2n\pi}{3}\right]\right)}{n^2} C_{snp}$$

where

$$C_{snp} = \frac{\left[2-np-4x^{np+2}+(np+2)x^4 \pm 2\left[\frac{2-np}{2+np}\right](1-x^{np+2})^2\left[\frac{R_{ao}}{R_s}\right]^{2np}\right]}{np[4-(np)^2]}$$

for $np \neq 2$

for $p=2$, $n=1$

$$C_{s2} = \frac{1}{4}x^4 \ln x + \frac{1-x^4}{16} \pm \frac{(1-x^4)^2}{32}\left[\frac{R_{ao}}{R_s}\right]^4$$

$$L_{fdn} = \frac{2\mu_o \ell_{fd} N_{ft} N_{np} \sin\left[\frac{n\theta_{wfe}}{2}\right]}{\theta_{wfe}(1-y^2)n^2p}\left[\frac{R_{fo}}{R_t}\right]^{np}\frac{(1-y^{np+2})}{(np+2)}\left[1\pm\left[\frac{R_t}{R_s}\right]^{2np}\right]$$

To get	Use Expression for	Replace	By
M_b	M_a	ϕ	$(\phi-2\pi/3)$
M_c	M_a	ϕ	$(\phi+2\pi/3)$
L_{bdn}	L_{adn}	ϕ	$(\phi-2\pi/3)$
L_{cdn}	L_{adn}	ϕ	$(\phi+2\pi/3)$
L_{aqn}	L_{adn}	$\cos np\phi$	$\sin np\phi$
L_{bqn}	L_{adn}	$\cos np\phi$	$\sin np(\phi-2\pi/3)$
L_{cqn}	L_{adn}	$\cos np\phi$	$\sin np(\phi+2\pi/3)$

1D Machine Rating Equations

The volt-ampere rating of a machine is given by

$$P = 3V_t I_a = 3E_f I_a \left(\frac{V_t}{E_f}\right) \tag{3}$$

where V_t, E_f, I_a, are RMS quantities.
The internal voltage E_f is given by

$$E_f = \frac{\omega_e M I_f}{\sqrt{2}} \tag{4}$$

and

$$\left(\frac{V_t}{E_f}\right) = \sqrt{1-x_a{}^2\cos^2\psi} - x_a\sin\psi \quad \text{(see Fig. 5)} \tag{5}$$

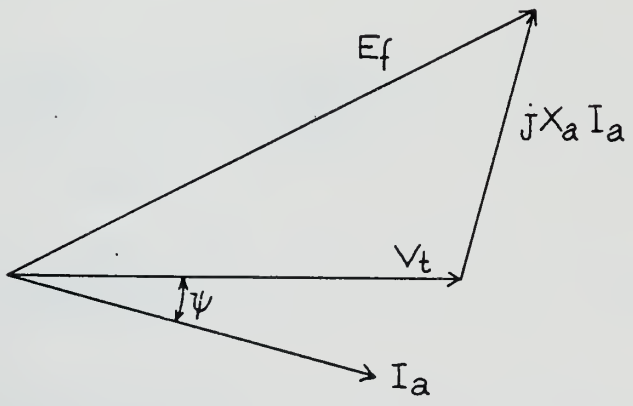

Figure 5
Voltage-current relationship

where x_a is synchronous reactance normalized to internal voltage

$$x_a = \frac{X_a I_a}{E_f} = \frac{W_e(L_a - L_{ab})I_a}{E_f} \qquad (6)$$

and

$$I_f = \frac{J_f \theta_{wfe} R_{fo}^2 (1-y^2)}{2N_{ft}}$$

$$I_a = \frac{J_a \theta_{wae} R_{ao}^2 (1-x^2)}{2N_{at}}$$

They may be combined to give

$$P = \frac{24}{\sqrt{2}\pi} W_e \mu_o l_m J_f J_a (1-y^{p+2}) R_{fo}^{p+2} R_{ao}^{2-p} \sin\left(\frac{\theta_{wae}}{2}\right) \sin\left(\frac{\theta_{wfe}}{2}\right) C_{lp}\left(\frac{V_t}{E_f}\right) \qquad (7)$$

where C_{lp} is given from Table 2

$$C_{lp} = \frac{[1-x^{2-p} \pm \left(\frac{2-p}{2+p}\right)(1-x^{2+p})\left(\frac{R_{ao}}{R_s}\right)^{2p}]}{P[4-p^2]} \qquad \text{for } p \neq 2$$

$$C_{lp} = [-\frac{1}{4} \ln x \pm \frac{1-x^4}{16}\left(\frac{R_{ao}}{R_s}\right)^4] \qquad \text{if } p=2$$

and x_a can be obtained by

$$x_a = \frac{1}{\sqrt{2}} \frac{l_a}{l_m} \frac{J_a}{J_f}\left(\frac{R_{ao}}{R_{fo}}\right)^{2+p} \frac{C}{\sin\left(\frac{\theta_{wae}}{2}\right)\sin\left(\frac{\theta_{wfe}}{2}\right)(1-y^{p+2})C_{lp}}$$

where C is given by

$$C = \sum_{n \text{ odd}} \frac{\sin^2\left(\frac{n\theta_{wae}}{2}\right)\left(1-\cos\left(\frac{2n\pi}{3}\right)\right)}{n^2} C_{snp}$$

and C_{snp} can be obtained from Table 2.
Transient reactances are calculated with the assumption that:

a) Field-winding flux is constant
b) Damper-winding current is zero

These reactances are[16,17]:

$$X_d' = X_d\left(1-\frac{3}{2}\cdot\frac{M^2}{(L_a-L_{ab})L_f}\right) \tag{8}$$

$$X_q' = X_d$$

where X_d is per unit synchronous reactance:

$$X_d = \frac{I_a X_a}{V_t} = X_a \frac{E_f}{V_t} \tag{9}$$

Subtransient reactances are calculated assuming that flux linked by the damper shield is constant. These are given by[16,17]

$$X_q'' = X_d'' = X_d\left(1-\frac{3}{2}\frac{M_s^2}{(L_a-L_{ab})L_{dl}}\right) \tag{10}$$

Since the shell is symmetric, direct and quadrature axis subtransient reactances are the same.

1E Machine Losses

There are mainly three different losses in synchronous machines[16]:

a) Current-conduction losses:

$$P = \frac{3\theta_{wae} J_a^2 R_{ao}^2 (1-x^2) \ell_c}{\sigma\lambda} \qquad (11)$$

b) Eddy-current losses:

$$P_{ec} = \frac{3\theta_{wae} R_{ao}^2 (1-x^2) w^2 \sigma\lambda B_{av}^2 \ell_{ed} d_w^2}{32} \qquad (12)$$

where B_{av}^2 is the mean-squared magnetic field seen by the armature conductors:

$$B_{av}^2 = \frac{1}{R_{ao}-R_{ai}} \int_{R_{ai}}^{R_{ao}} B_{rfo}^2 . dr \qquad (13)$$

where B_{rfo} is given in Table 1. If the first harmonic of B_{rfo} is considered, for a two-pole (one pole pair) iron shielded machine:

$$B_{rfo} = \frac{2\mu_o J_f \sin\left(\frac{\theta_{wfe}}{2}\right)}{3\pi} r \left(\frac{R_{fo}}{r}\right)^3 (1-y^3)\left[1+\left(\frac{r}{R_s}\right)^2\right]$$

When this is substituted into (13):

$$B_{av}^2 = \left[\frac{1}{R_{ao}-R_{ai}}\right]\left[\frac{2\mu_o J_f R_{fo}^3 \sin\left(\frac{\theta_{wfe}}{2}\right)(1-y^3)}{3}\right]^2 \cdot$$

$$\left[\frac{1}{3R_{ai}^3}(1-x^3)+\frac{(1-x)}{R_s^2}\left(\frac{2}{R_{ai}}+\frac{R_{ao}}{R_s^2}\right)\right] \qquad (14)$$

c) Shield losses:

If an image shield is used, circulating currents will produce losses:

$$P_{sh} = \frac{\pi B_{\theta s}^{2} R_s \ell_{sh}}{\mu_o^2 \sigma_s \delta_s} \qquad (15)$$

where $B_{\theta s}$ is B_θ evaluated at shield inside radius, and δ_s is the skin depth of the shield material.

If an iron shield is used, eddy-currents and hysterisis will produce losses:

$$P_{sh} = \pi(R_{os}^{2}-R_s^{2})\ell_{sh}\, \rho_{sh}\, d_{sh} \qquad (16)$$

where d_{sh} is shield dissipation per unit mass of shield material. The effective lengths will be discussed in Appendix B.

1F Fault Effects

Although elimination of iron reduces the machine volume and weight, it degrades the transient behaviour of superconducting machines. Large fault torques and stresses will be imposed upon the field winding. In addition to fault loading, there will be heat dissipation and field current rise, which may drive superconducting field winding normal. The protection needed will be provided by a suitable shield around the field winding. The expressions for fault loadings under various fault conditions are derived in references 1 and 18. For us the maximum values are important in order to design a machine which can withstand such loads.

The maximum radial loads imposed upon the primary shield will be under three phase short circuit from load. These are given by[1,18]:

$$\sigma_r = \frac{1}{2}\mu_o(H_{\theta o}^2 - H_{\theta i}^2) \qquad (17)$$

where H_0 and H_i are the fields outside and inside the shell respectively after the fault:

$$H_{\theta 0} = -H_a[\cos(wt_f+\phi_f-p\theta)-\cos(\phi_f-p\theta)]$$
$$-_fHa[\cos(wt_f+\phi_f-p\theta)-\cos(\phi_f-p\theta)]$$
$$-H_{\theta f}\cos(wt_f+\phi_f-p\theta) \qquad (18)$$

and

$$H_{\theta i} = H_{\theta f}\cos(wt_f+\phi_f-p\theta)$$

where

$$f = \frac{1\mp\left[\frac{R_t}{R_s}\right]^{2p}}{1\pm\left[\frac{R_t}{R_s}\right]^{2p}}$$

and H_a is the armature field at primary shield radius:

$$H_a = \frac{3\sqrt{2}}{\pi} J_a \frac{e_f''}{X_d''} \sin\left(\frac{\theta_{wae}}{2}\right) R_t \left(\frac{R_t}{R_{ao}}\right)^{p-2} \frac{\left[1-x^{2-p} \pm \left(\frac{2-p}{2+p}\right)(1-x^{2+p})\left(\frac{R_{ao}}{R_s}\right)^{2p}\right]}{(2-p)}$$

if $p \neq 2$ (19a)

$$H_a = \frac{3\sqrt{2}}{2\pi} J_a \frac{e_f''}{X_d''} \sin\left(\frac{\theta_{wae}}{2}\right) R_t \left[-\ln x \pm \frac{1}{4}(1-x^4)\left(\frac{R_{ao}}{R_s}\right)^9\right] \quad (19b)$$

if $p=2$

and H_f is the field generated by field windings at primary shield radius:

$$H_{\theta f} = \frac{2J_f \sin\left(\frac{\theta_{wfe}}{2}\right)}{\pi(2+p)} R_t \left(\frac{R_{fo}}{R_t}\right)^{2+p} (1-y^{p+2})\left[1 \pm \left(\frac{R_t}{R_s}\right)^{2p}\right] \quad (20)$$

It should be noted that only the first harmonic fields have been taken into account.

When equations (18), (19), and (20) are combined with (17) and the maximum stress evaluated when $wt_f = \pi$,

$$\sigma_r = 2\mu_o H_a (1+f)[H_a(1+f)+H_{f\theta}]\cos^2(p\theta - \phi_f) \quad (21)$$

The maximum torque will be applied on the primary shield under line-to-line short circuit from load. This torque is given by[1,18]:

$$T = \frac{e_f''^2}{X_d''} [\cos wt\ (\sin wt_0 - \sin wt)] \quad (22)$$

and the maximum value will occur at $wt_0 = \pi/2$, for which

$$T_{max} = 1.3 \frac{e_f''^2}{X_d''} \quad (23)$$

In above derivations a factor e_f'', voltage behind the subtransient reactance, was introduced to correct fault loads from open circuit to load in an approximate fashion. Figure 6 shows a method to calculate e_f'' from which

$$e_f'' = \frac{E_f''}{V_t} = \sqrt{(1+X_d'' \sin\psi)^2 + (X_d'' \cdot \cos\psi)^2} \qquad (24)$$

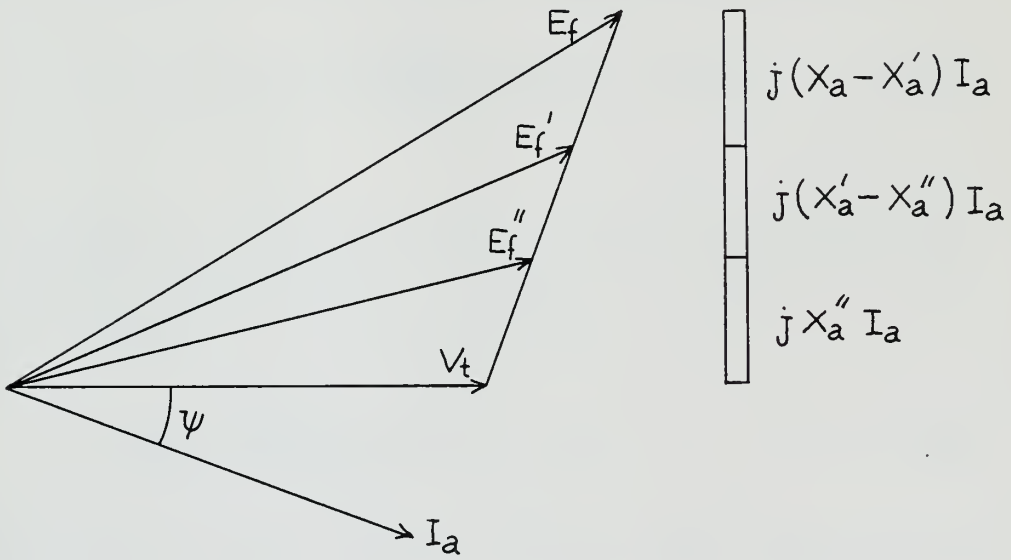

Figure 6
Vector Diagram of Internal, Terminal and Reaction Voltages

Since, primary shield will not be strong enough to resist fault loadings, it must be supported by a shield structure. Stresses induced under radial and torque loads are derived in Appendix A.

Under fault conditions, the superconducting field winding may be driven normal, due to the heat dissipation and the field current rise. Perhaps the most important one is the field current rise[18] in both dc and ac levels. Allowable field current rise will depend on the rated operating point with respect to superconductor short sample curve. Figure 7 illustrates the allowable field current rise for a given operating point. Ac component of the field current rise will be small[18] compared to the dc component and may be neglected. Field current will rise exponentially and its final value will depend on primary shield time constant, machine reactances and circuit breaker opening time[1,18]:

$$i_f = i_{fo}\left[1 + \frac{X_d - X_d'}{X_d'}\left(1 - e^{-t/T_d''}\right)\right] \qquad (25)$$

where i_f and i_{fo} are the instant and initial values of field current respectively; and, T_d'' is related to the primary shield time constant by[18],

$$T_d'' = \left(\frac{X_d''}{X_d'}\right)\left(\frac{X_d' - X_d''}{X_d - X_d''}\right) T_{sl} \qquad (26)$$

and for a thin primary shield, shield time constant[18,16]:

$$T_{sl} = \frac{1}{2p}\mu_o \sigma\, t_s\, R_t\left[1 \pm \left(\frac{R_t}{R_s}\right)^{2p}\right] \qquad (27)$$

This time constant will also determine the machine swings under transient conditions, but this was not included in this study.

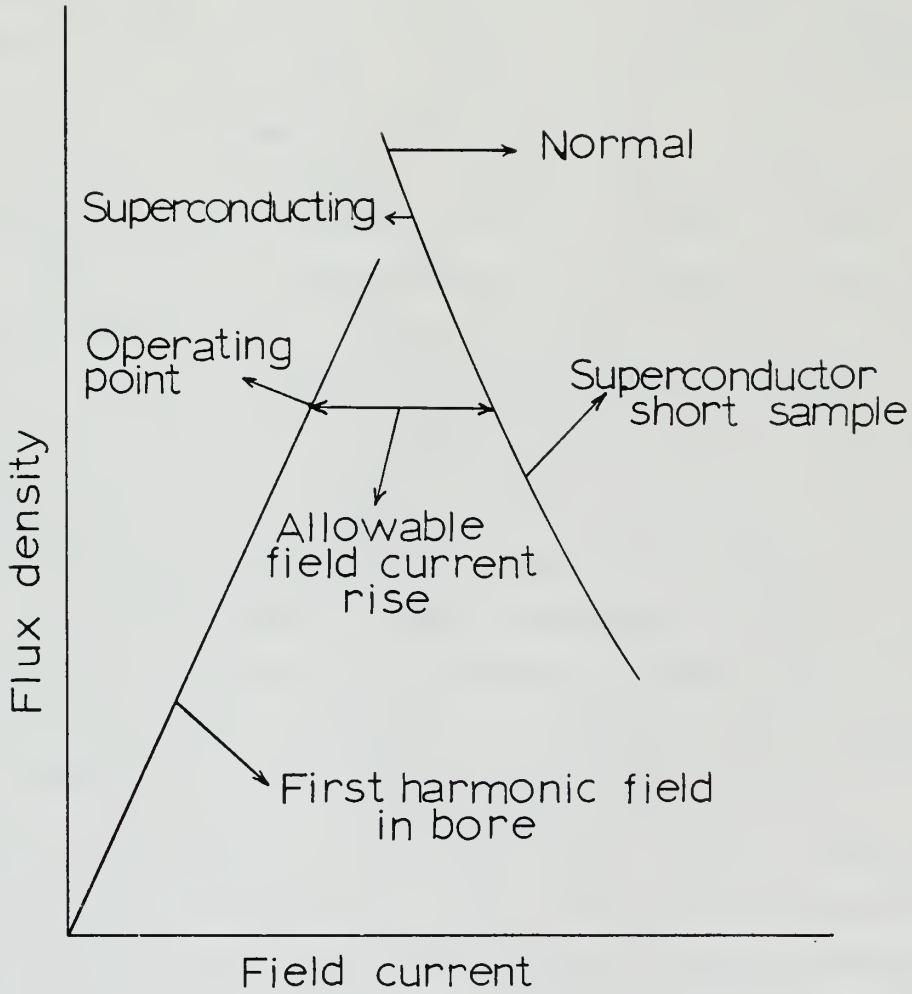

Figure 7
Allowable Field Current Rise

1G Design Constraints

A superconducting coil is characterized by its short sample test curve. At a given operating temperature, the relation between flux density and current density which can be carried without driving superconductor normal, constitutes such a curve. Any chosen operating point should be to the left of this curve. In order to provide stability against disturbances of electrical, thermal, or mechanical nature which may occur, a material of high electrical and thermal conductivity is included in the conductor. Copper is usually used for this purpose. High-purity aluminum has not been accepted because of the problem of making a metallurgical bond with the superconductor although it has higher electrical conductivity. Recently a metallurgical bond has been made[22] but the brittle nature of it still limits aluminum as a stabilizer. Figure 8 shows Nb Ti superconductor short sample test data, with the state of the art line given in reference 21. To the right of this line small disturbance may drive superconductor to normal, according to the stability criteria given in this reference. Although such a line is quite arbitrary, it defines a region which is experienced with other magnets. It should be pointed out that the higher flux densities are possible with Nb_3 Sn conductors, but they are more expensive than Nb Ti conductors and cannot be fabricated into complex windings.

Another major limitation comes from the saturation considerations of the iron shield used to confine magnetic fields inside the machine volume. The shield may be locally saturated or the maximum flux density carried by the shield may exceed saturation flux density of the iron. These considerations will be discussed in detail in Appendix B when the computer program is described.

Armature current density will be determined by the losses and cooling method employed. A figure of 3.0×10^6 amp/m^2 could be accepted for a nitrogen cooled armature.

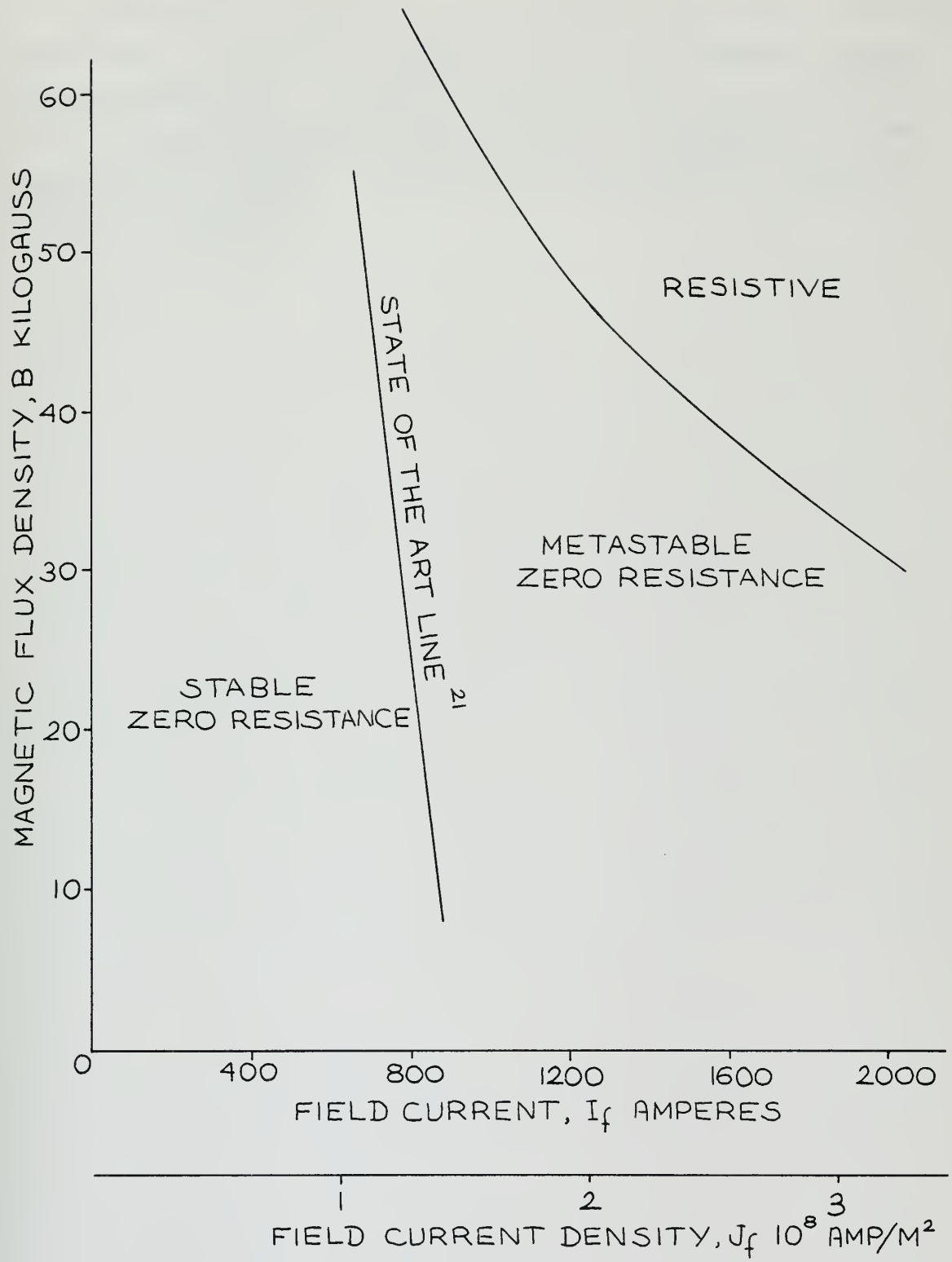

Figure 8

Superconductor Short Sample Test Data

Structural integrity of the machine structure will also constitute a problem especially when it is degraded under fault conditions. The most critical part of the machine will be the shield structure and must be designed to take large fault loadings. This will be discussed in Appendix A and B, in detail.

Chapter 2
RESULTS

2A Parameters Used in the Design Study

For the purpose of this study, calculations were performed for a 20,000 HP, two-pole synchronous generator. Input parameters to the computer program are given in Table 3. First harmonic field in the bore of the field winding is shown in Figure 9 along with the superconductor short sample test curve. Shield structure is assumed to be stainless steel and low values of working stresses are chosen due to the fact that heat dissipation will degrade material properties. The 120 degree field winding angle has an advantage of eliminating third harmonic component of field thus preventing flow of third harmonic currents in delta connected machines. In addition to the input parameters given in Table 3, field winding inside radius of 2.76 inches and outside radius of 5.0 inches were chosen, and the iron shield was assumed to be on the armature end turns (t = 0).

Although the program could be run several times with different field winding radii and input parameters to get absolute minimum weight and volume machine, this process was omitted here and only a design for a given set of input parameters defined in Table 3, was obtained.

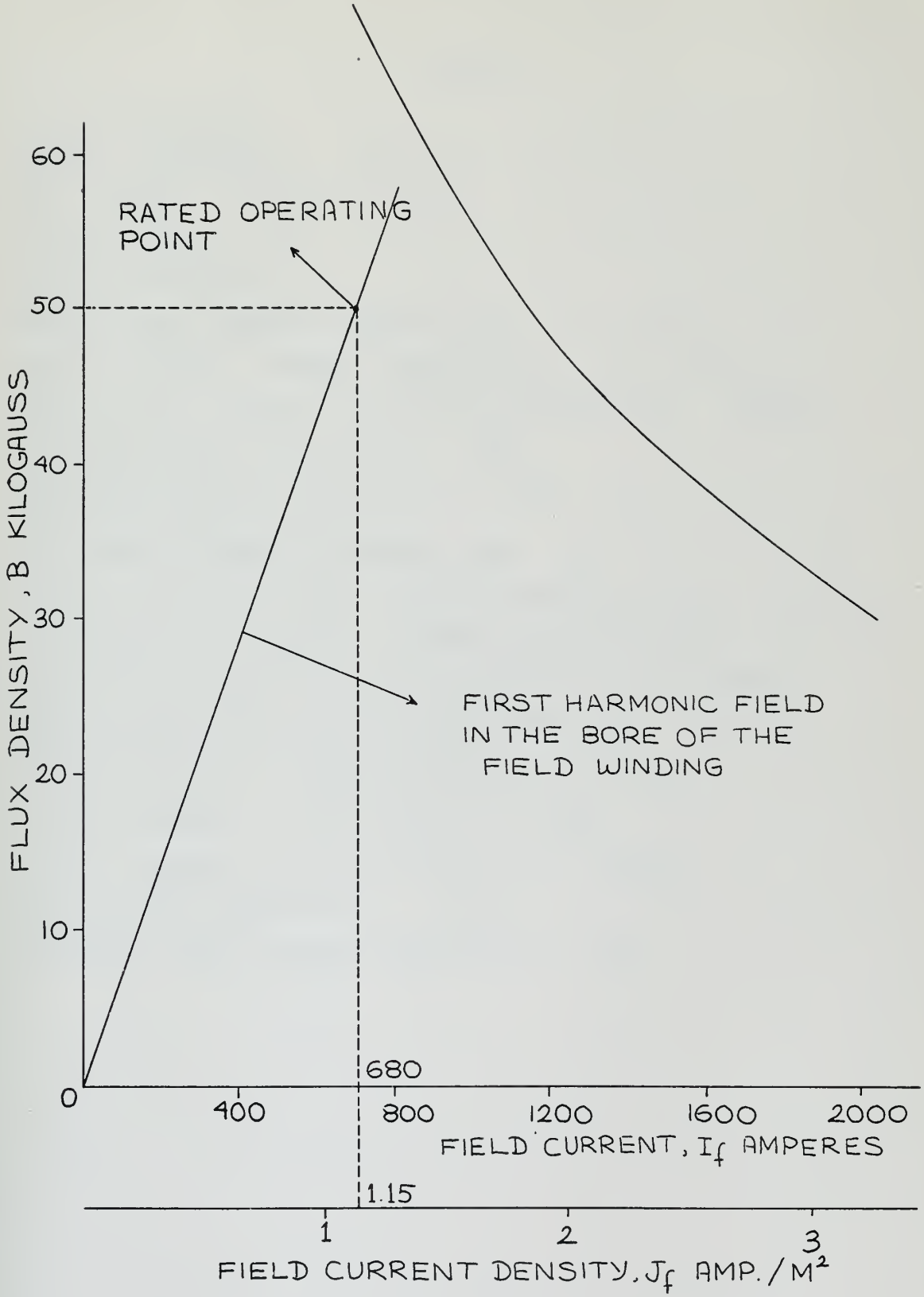

Figure 9

First Harmonic Field in the Bore of the Field Winding

TABLE 3

DESIGN CONSTANTS
DESIGN HORSEPOWER= 20450.25
MVA RATING= 15.25
POWER FACTOR=1.00
DESIGN RPM=3600.0
RATED FIELD CURRENT DENSITY=1.15 10 8 A/M2
RATED ARMATURE CURRENT DENSITY=3.00 10 6 A/M2
MAXIMUM FLUX DENSITY IN FIELD WINDING=5.00 TESLAS
FIELD WINDING ANGLE=120.00 DEG.
ARMATURE WINDING ANGLE=60.00 DEG.
ARMATURE SPACE FACTOR=0.27
ARMATURE FILAMENT DIAMETER=0.040 IN.
YOUNG MODULUS OF SHIELD SUPPORT MATERIAL=29.0 10 6 PSI
POISSON RATIO OF SHIELD SUPPORT MATERIAL=0.300
ELECTRICAL CONDUCTIVITY OF SHIELD=6.0 10 7 MHO/M
DENSITY OF SHIELD SUPPORT MATERIAL=0.290 LBS/IN3
WORKING STRESS IN TENSION=50000.0 PSI.
WORKING STRESS IN COMPRESSION=50000.0 PSI.
WORKING STRESS IN SHEAR=30000.0 PSI.
CIRCUIT BREAKER OPENNING TIME=10.0 CYCLES
RATED FIELD CURRENT=680.0 AMP.
ALLOWABLE FIELD CURRENT RISE=420.0 AMP.

2B Effect of Primary Shield Location

Figure 10 shows the effect of primary shield location where the induced currents flow under fault conditions, for different air gap lengths. Calculations are done for the same set of input parameters as defined in Table 3. The case where the primary shield is inside the shield structure, produces less radial stresses than the case where primary shield is outside the shield structure, under three phase short circuit from load, thus may require less shield structure and airgap length and therefore less machine volume. Two computer outputs given in Tables 4 and 5, show this effect. As can be seen, the results are not very different from each other. Although the case where primary shield is inside shield structure gives smaller machine volume and length, the direct exposure of the shield structure to the trapped magnetic fields may induce higher heat dissipation thus increasing the refrigeration power required.

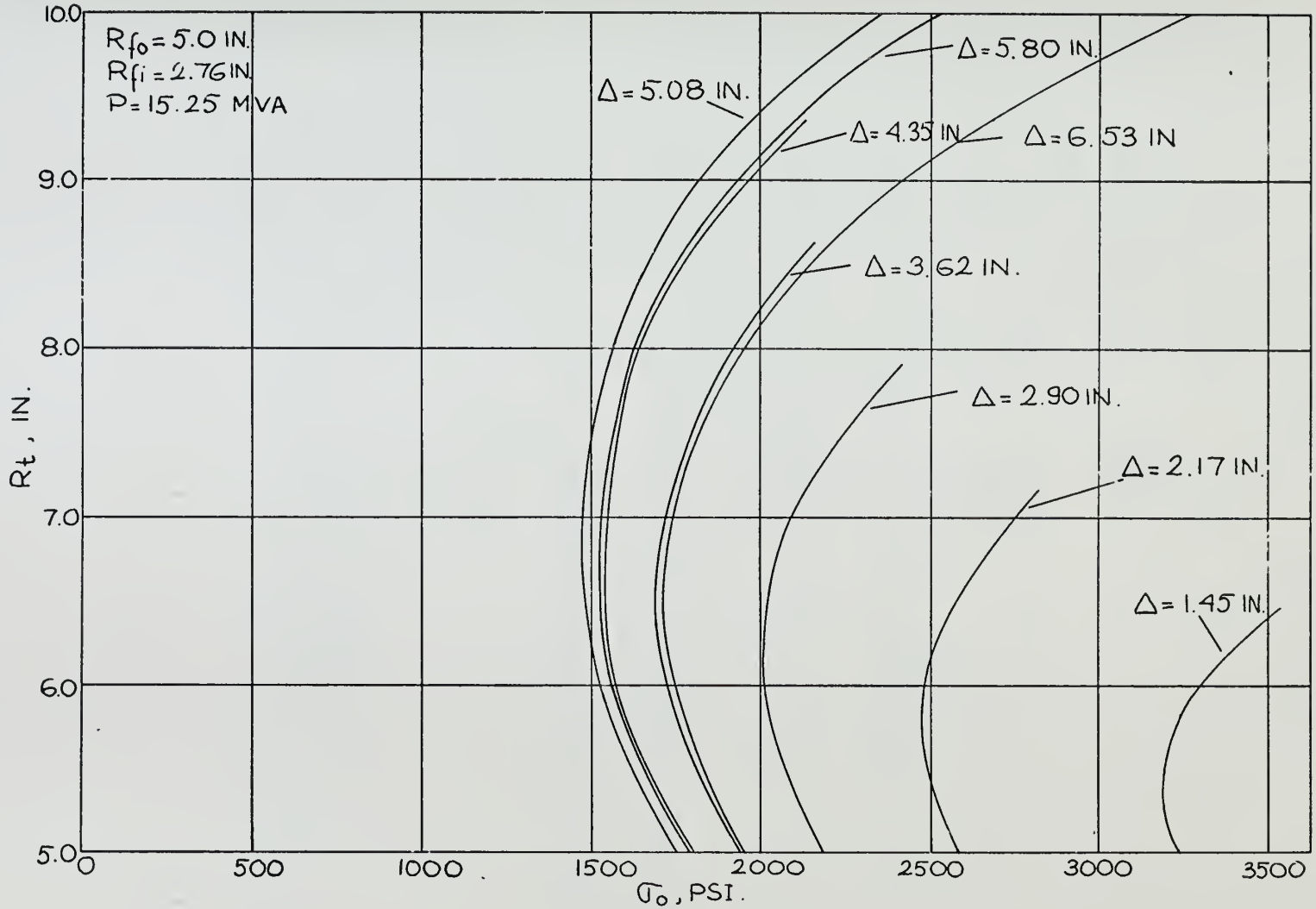

Figure 10

Effect of Primary Shield Location

TABLE 4

FIELD WINDING OUTSIDE RADIUS= 5.000 IN.
FIELD WINDING INSIDE RADIUS= 2.760 IN.
ARMATURE INSIDE RADIUS= 6.451 IN.
ARMATURE OUTSIDE RADIUS= 9.354 IN.
SHIELD INSIDE RADIUS= 12.257 IN.
SHIELD OUTSIDE RADIUS= 19.887 IN.
TOTAL LENGTH=58.848 IN.
STRAIGHT SECTION LENGTH= 27.237 IN.
MACHINE VOLUME= 42.313 FT 3
WEIGHT OF ACTIVE PARTS= 16418.903 LBS.
PRIMARY SHIELD IS OUTSIDE THE SHIELD STRUCTURE
AIR GAP LENGTH= 1.4514 IN.
PRIMARY SHIELD OUTSIDE RADIUS= 6.364 IN.
SHIELD STRUCTURE OUTSIDE RADIUS= 6.364 IN.
PRIMARY SHIELD THICKNESS= 0.0 IN.
SHIELD STRUCTURE THICKNESS= 1.3410 IN.
SHIELD DEFLECTION TOWARDS FIELD WINDING UNDER THREE PHASE FAULT= 0.0220 IN.
SHIELD DEFLECTION TOWARDS ARMATURE WINDING UNDER THREE PHASE FAULT=-0.0205 IN.
SYNCHRONOUSREACTANCE P.U.=0.2533
TRANSIENT REACTANCE P.U.=0.1875
SUBTRANSIENT REACTANCE P.U.=0.1283
MACHINE LOSSES PERCENT OF MACHINE RATING=0.751
MAX. RADIAL STRESS UNDER THREE PHASE FAULT= 3482.8 PSI
MAXIMUM TORQUE UNDER LINE TO LINE SHORT CIRCUIT FROM LOAD P.U.= 10.303

TABLE 5

FIELD WINDING OUTSIDE RADIUS= 5.000 IN.
FIELD WINDING INSIDE RADIUS= 2.760 IN.
ARMATURE INSIDE RADIUS= 6.306 IN.
ARMATURE OUTSIDE RADIUS= 9.282 IN.
SHIELD INSIDE RADIUS= 12.257 IN.
SHIELD OUTSIDE RADIUS= 19.887 IN.
TOTAL LENGTH= 57.950 IN.
STRAIGHT SECTION LENGTH= 26.773 IN.
MACHINE VOLUME= 41.667 FT 3
WEIGHT OF ACTIVE PARTS= 16169.683 LBS.
PRIMARY SHIELD IS INSIDE THE SHIELD STRUCTURE
AIR GAP LENGTH= 1.3063 IN.
PRIMARY SHIELD OUTSIDE RADIUS= 5.026 IN.
SHIELD STRUCTURE OUTSIDE RADIUS= 6.2941 IN.
PRIMARY SHIELD THICKNESS= 0.0 IN.
SHIELD STRUCTURE THICKNESS= 1.2680 IN.
SHIELD DEFLECTION TOWARDS FIELD WINDING UNDER THREE PHASE FAULT= 0.0245 IN.
SHIELD DEFLECTION TOWARDS ARMATURE WINDING UNDER THREE PHASE FAULT=-0.0229 IN.
SYNCHRONOUS REACTANCE P.U.=0.2519
TRANSIENT REACTANCE P.U.=0.1849
SUBTRANSIENT REACTANCE P.U.=0.1657
MACHINE LOSSES PERCENT OF MACHINE RATING=0.749
MAX. RADIAL STRESS UNDER THREE PHASE FAULT= 3377.9 PSI.
MAXIMUM TORQUE UNDER LINE TO LINE SHORT CIRCUIT FROM LOAD P.U.=8.061

2C Comparison Between 20,000 HP Conventional Generator and a Superconducting Generator

The results obtained in previous section are compared with a 20,000 HP conventional propulsion generator[13]. Figure 11 shows such a comparison in machine dimensions. An additional 15,000 lbs are added to the weight of the superconducting generator in order to take account of the machine casing, bearings excitation system, etc. Table 6 lists some of the information available about the conventional generator. Unavailability of additional information limits comparison in machine dimensions and weight. As far as refrigeration weight and volume are concerned, there will not be anything to say unless rotor is structurally and mechanically designed. In addition refrigeration system may be integrated to provide for other superconducting electric machinery.

TABLE 6

20,000 HP Conventional Generator Characteristics

	Maximum Continuous Rating	2 Minute Capacity
KVA	15,250	
RPM	3,600	900
Volts	4,700	823
Power Factor	1.0	
Frequency, Hz	60	
Amperes		300% Max.

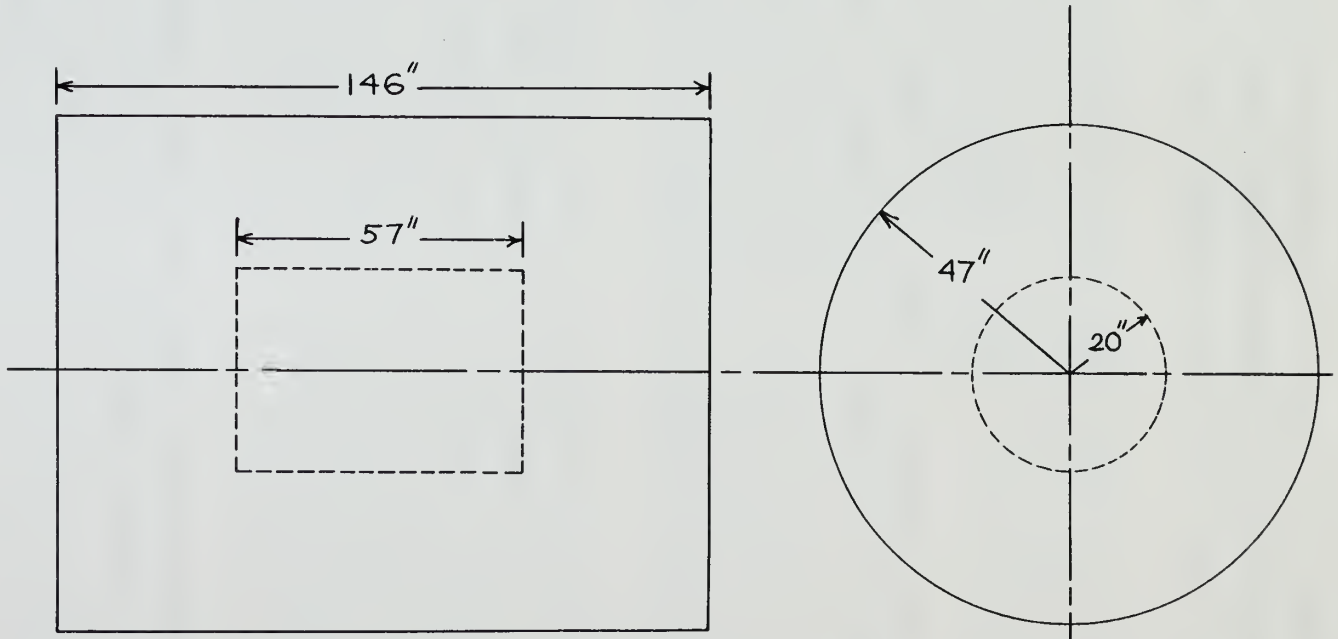

Figure 11
Comparison Between 20,000 HP Conventional Generator
and a Superconducting Generator

Chapter 3
CONCLUSIONS AND RECOMMENDATIONS

One major conclusion that can be drawn from the previous results is that, superconducting machines can be built to withstand fault loadings and still have low weight and volume.

Since most of the weight comes from the iron shield, replacement of it by a conductive image shield may lead to additional weight savings, although image shield may introduce additional losses.

Replacement of copper by aluminum as a stabilizer will also reduce field winding weight if a suitable fabrication technique can be found.

Conversion of the computer program for many pole machines will increase its usefulness and provide information about low speed (100-200RPM) synchronous propulsion motors.

Although a simple technique could be employed which changes input parameters systematically and gives direction towards minimum weight or minimum volume machine, it is the belief of the author that such technique would require a great amount of computer time and money. Furthermore, minimum weight or volume machine may not be best as far as rotor mechanical design and refrigeration input are concerned.

Perhaps, the most questionable assumption is that the weight densities for individual machine parts are uniform, especially for the rotor structure. Correct estimation of rotor weight can be done only by structural and mechanical design. Critical speeds of the rotor may not be acceptable and in that case rotor structure or length should be modified. Rotor lenght should be increased as much as possible in order to increase thermal resistance and thereby

reduce heat leak into cold region. Critical speeds will, however, limit the rotor length. Inclusion of above considerations will require longer computation time but may give more useful information about superconducting machines.

Appendix A

SHIELD DEFLECTION AND STRESSES UNDER FAULT CONDITIONS

It has been assumed that only the shield structure will be effective for carrying fault loads. Figure A-1 shows radial loads imposed upon simply supported shield structure under three phase fault, with the addition of centrifugal loading. It is easier to separate these two loadings and superimpose them after each solution is obtained separately.

Reference 19 gives three differential equations for deflections:

$$\frac{\partial^2 u}{\partial x^2} + \frac{1-\nu}{2a^2}\frac{\partial^2 u}{\partial \theta^2} + \frac{1+\nu}{2a}\frac{\partial^2 v}{\partial x \partial \theta} - \frac{\nu}{a}\frac{\partial w}{\partial x} = 0 \qquad \text{(A-1a)}$$

$$\frac{1+\nu}{2a}\frac{\partial^2 u}{\partial x \partial \theta} + \frac{1-\nu}{2}\frac{\partial^2 v}{\partial x^2} + \frac{1}{a^2}\frac{\partial^2 v}{\partial \theta^2} - \frac{1}{a^2}\frac{\partial w}{\partial \theta} + \frac{h^2}{12a^2}$$

$$\left[\frac{\partial^3 w}{\partial x^2 \partial \theta} + \frac{\partial^3 w}{a^2 \partial \theta^3}\right] + \frac{h^2}{12a^2}\left[\frac{1-\nu}{2}\frac{\partial^2 v}{\partial x^2} + \frac{\partial^2 v}{a^2 \partial \theta^2}\right] = 0 \qquad \text{(A-1b)}$$

$$\nu\frac{\partial u}{\partial x} + \frac{\partial v}{a\partial \theta} - \frac{w}{a} - \frac{h^2}{12}\left[a\frac{\partial^4 w}{\partial x^4} + \frac{2}{a}\frac{\partial^4 w}{\partial x^2 \partial \theta^2} + \frac{\partial w^4}{a^3 \partial \theta^4}\right.$$

$$-\frac{h^2}{12}\left[\frac{2-\nu}{a}\frac{\partial^3 v}{\partial x^2 \partial \theta} + \frac{1}{a^3}\frac{\partial^3 v}{\partial \theta^3}\right] + \frac{ap_3(1-\nu^2)}{Eh} = 0 \qquad \text{(A-1c)}$$

Simply supported boundary conditions imply that,

$$\text{at } x = 0 \text{ and } x = L$$

$$v = 0,\ w = 0,\ N_x = 0,\ M_x = 0$$

These boundary conditions can be satisfied if one chooses :

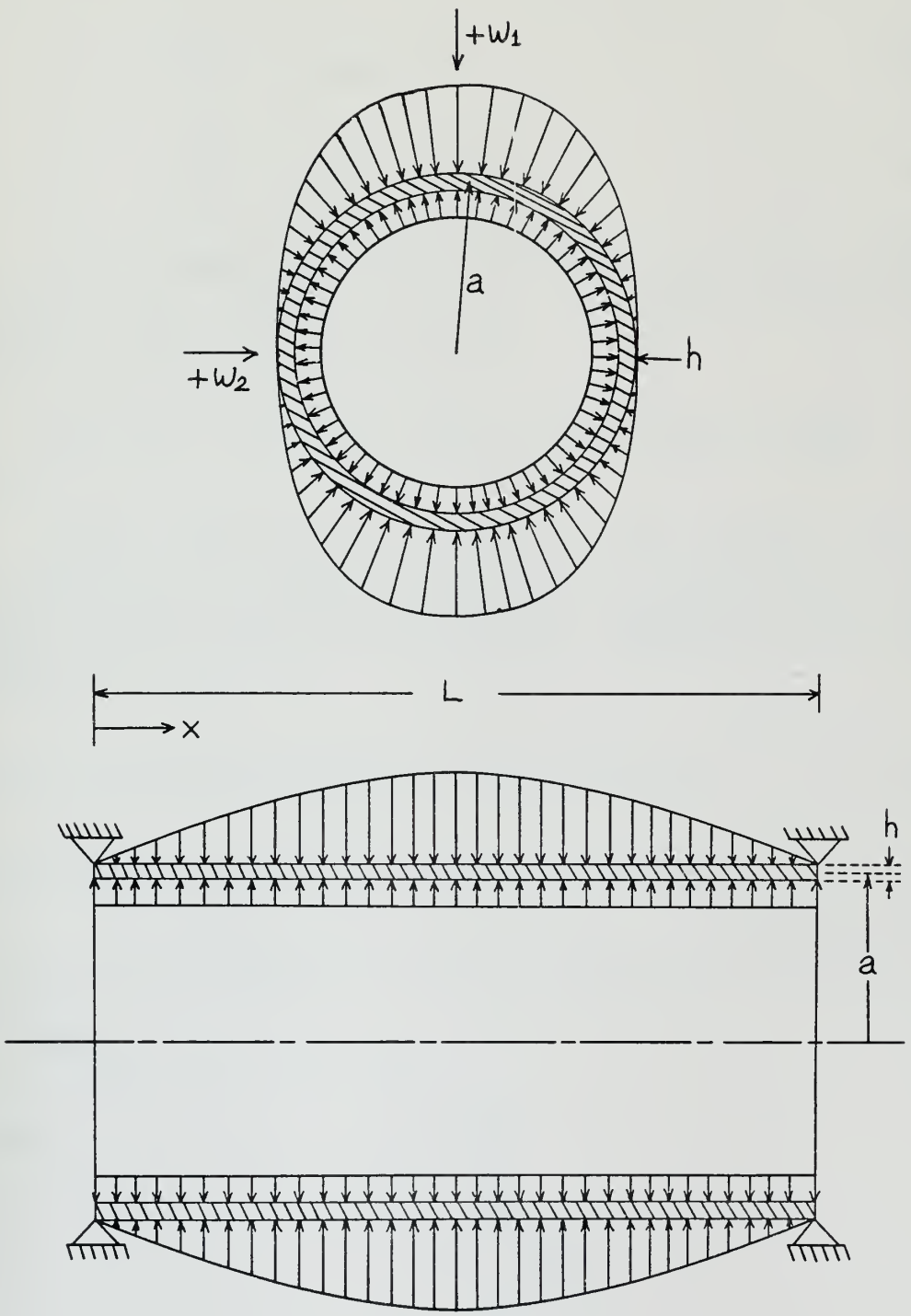

Figure A-1

Three Phase Fault Radial and Centrifugal Loading on Shield Structure

$$u = \cos\frac{\pi x}{L} \Sigma A_n \cos n\theta \qquad \text{(A-2a)}$$

$$v = \sin\frac{\pi x}{L} \Sigma B_n \sin n\theta \qquad \text{(A-2b)}$$

$$w = \sin\frac{\pi x}{L} \Sigma C_n \cos n\theta \qquad \text{(A-2c)}$$

It was shown in Chapter 2-F that the radial stresses depend on the angular position along the circumference. They are given by equation 21.

$$P_3 = \sigma_r = \sigma_o \cos^2\theta = \frac{\sigma_o}{2}(1 + \cos 2\theta) \times \sin\frac{\pi x}{L} \qquad \text{(A-3)}$$

When equations (A-2) and (A-3) are combined with (A-1), and the last two terms neglected in equation (A-1b) because they will be small for thin shells compared to the other terms,

$$A_n[2\pi^2+(1-\nu)\lambda^2n^2]-B_n[(1+\nu)\lambda\pi n]+C_n[2\nu\lambda\pi]=0 \qquad \text{(A-4a)}$$

$$A_n[3(1+\nu)\pi n\lambda]-B_n[3(1-\nu)\pi^2+6\lambda^2n^2]+C_n[6\lambda^2n]=0 \qquad \text{(A-4b)}$$

$$A_n[\nu\pi 3\lambda]-B_n\, n\lambda^2\left[3+\eta^2[(2-\nu)\pi^2+\lambda^2n^2]\right]+C_n[3\lambda^2+\eta^2(\pi^2+\lambda^2n^2)^2]$$

$$= \frac{L^4\eta^2}{D}P_n \qquad \text{(A-4c)}$$

where

$$\lambda = \frac{L}{r}$$

$$\eta = \frac{h}{2L}$$

$$D = \frac{Eh^3}{12(1-\nu^2)}$$

and for n=0 and 2, $P_o=P_2=\frac{\sigma_o}{2}$, the result which comes directly from equation (A-3)

The coefficients obtained by solution of equation (A-4) are too complicated to write explicitly. The results are summarized in Table A-1. The stresses can be obtained by,

$$\sigma_x = \frac{E}{1-\nu^2} [\varepsilon_x+\nu\varepsilon_\theta-z(X_x+\nu X_\theta)] \qquad \text{(A-5a)}$$

$$\sigma_\theta = \frac{E}{1-\nu^2} [\varepsilon_\theta+\nu\varepsilon_x-z(X_\theta+\nu X_x)] \qquad \text{(A-5b)}$$

$$\tau_{x\theta} = \frac{E}{2(1+\nu)} (\delta-2zX_{x\theta}) \qquad \text{(A-5c)}$$

where

$$\varepsilon_x = \frac{\partial u}{\partial x} \qquad \text{(A-6a)}$$

$$\varepsilon_\theta = \frac{1}{a} \frac{\partial \upsilon}{\partial \theta} - \frac{w}{a} \qquad \text{(A-6b)}$$

$$\delta = \frac{\partial \upsilon}{\partial x} + \frac{1}{a} \frac{\partial u}{\partial \theta} \qquad \text{(A-6c)}$$

$$X_x = \frac{\partial^2 w}{\partial x^2} \qquad \text{(A-6d)}$$

$$X_\theta = \frac{1}{a} \frac{\partial}{\partial \theta} \left(\frac{\upsilon}{a} + \frac{1}{a} \frac{\partial w}{\partial \theta}\right) \qquad \text{(A-6e)}$$

$$X_{x\theta} = \frac{1}{a} \left(\frac{1}{2} \frac{\partial \upsilon}{\partial x} + \frac{\partial^2 w}{\partial x \partial \theta}\right) \qquad \text{(A-6f)}$$

and z is the distance from the mid-surface (positive towards the axis of the shell). Equation (A-6) can be combined with equation (A-5) to give stresses in axial and circumferential directions.

TABLE A-1

Solution of equation A-4

$$A_o = -\frac{\nu\lambda}{\pi} C_o$$

$$B_o = 0$$

$$C_o = \frac{L^4\eta^2\sigma_o}{2D[3\lambda^2(1-\nu^2)+\eta^2\pi^4]}$$

$$A_2 = -B_2 \frac{\left[\frac{12\lambda^2(1+\nu)}{\nu} - 3(1-\nu)\pi^2-24\lambda^2\right]}{\left[6(1+\nu)\pi\lambda-\frac{12\lambda}{\nu\pi}[\pi^2+(1-\nu)2\lambda^2]\right]}$$

$$B_2 = \frac{L^4\eta^2\sigma_o}{2D} \cdot \left[6(1+\nu)\pi\lambda-\frac{12\lambda}{\nu\pi}[\pi^2+(1-\nu)2\lambda^2]\right] / \left[\left[\left(\frac{1+\nu}{\nu}\right)[3\lambda^2+\eta^2 (\pi^2+4\lambda^2)^2]-2\lambda^2[3+\eta^2[(2-\nu)\pi^2+4\lambda^2]]\right] \cdot \left[6(1+\nu)\pi\lambda-\frac{12\lambda}{\nu\pi} [\pi^2+(1-\nu)2\lambda^2]\right]-\left[\frac{12\lambda^2(1+\nu)}{\nu} -3(1-\nu)\pi^2-24\lambda^2\right] \cdot \left[3\nu\pi\lambda- [2\pi^2+(1-\nu)4\lambda^2] \cdot [3\lambda^2+\eta^2(\pi^2+4\lambda^2)^2]/[2\nu\lambda\pi]\right]\right]$$

$$C_2 = \frac{B_2 \cdot [2(1+\nu)\lambda\pi]-A_2 \cdot [2\pi^2+(1-\nu)4\lambda^2]}{2\nu\lambda\pi}$$

Since the shield will rotate with field winding, centrifugal stresses will be induced with associated deflections. The centrifugal loading may be considered as loading due to uniform internal pressure given by:

$$P = \frac{\rho w^2 ah}{g} \qquad \text{(A-7)}$$

Reference 19 gives the solution for a circular cylindrical shell with a uniform internal pressure with ends simply supported:

$$w = -\frac{PL^4}{G4D\alpha 4}\left|1 - \frac{2\sin\alpha \cdot \sinh\alpha}{\cos 2\alpha + \cosh 2\alpha} \cdot \sin\beta(x-\frac{L}{2}) \cdot \sinh\beta(x-\frac{L}{2})\right.$$

$$\left. - \frac{2\cos\alpha \cdot \cosh\alpha}{\cos 2\alpha + \cosh 2\alpha} \cdot \cos\beta(x-\frac{L}{2}) \cdot \cosh\beta(x-\frac{L}{2})\right| \qquad \text{(A-8)}$$

where $$\beta = \sqrt[4]{\frac{3(1-\nu^2)}{a^2h^2}}$$

and $$\alpha = \frac{\beta L}{2}$$

Equation (A-8) is the deflection in vertical direction. From symmetry, the component ν of the displacement in the circumferential direction vanishes. The expressions for the strain components then become

$$\varepsilon_x = \frac{du}{dx} \qquad \text{(A-9a)}$$

$$\varepsilon_\theta = -\frac{w}{a} \qquad \text{(A-9b)}$$

and it can be shown that[19]

$$\frac{du}{dx} = \nu \frac{w}{a} \qquad \text{(A-10)}$$

Equations (A-5), (A-6),(A-7), (A-8), (A-9), (A-10) and Table A-1 can be combined to get total deflections and stresses along the shell at any point on circumference. The component w of the displacement will be maximum at midlength (x=L/2) when $\theta=0$ and $\theta=\pi/2$ denoted by w_1 and w_2 respectively. These two deflections will determine the required airgap along with shield thickness. If the material properties are chosen, it is possible to calculate stresses at these points, top and bottom surfaces. Since the shear stresses will be zero, these are actually principal stresses. Maximum shear stresses can be obtained by,

$$\tau_{x\theta} = \frac{\sigma_x - \sigma_\theta}{2} \qquad \text{(A-11)}$$

Under line-to-line short circuit from load, large fault torques are applied on the shield. The magnitude of these torques is given by[23]. The shield structure must be strong enough to carry these stresses. For the shear stress in the shell, according to the maximum shear theory[23]

$$(\tau_{x\theta})_{max} = 2\left[\left(\frac{\sigma_\theta}{2}\right)^2 + (\tau_{x\theta})^2\right]^{1/2} \qquad \text{(A-12)}$$

in this case σ_θ will be assumed to consist of centrifugal stresses only, that is,

$$\sigma_\theta = \frac{\rho w^2 r^2}{g} \qquad \text{(A-13)}$$

and

$$\tau_{x\theta} = \frac{2R_{so}T}{\pi(R_{so}^4 - R_{si}^4)} \qquad \text{(A-14)}$$

Equations (A-13), (A-14), and (A-12) may be combined to give maximum shear stresses.

Application of this fault torque may cause buckling of shield. Reference 20 gives criteria for critical buckling stresses.

$$\tau_{cr} = 0.85\ (\pi^2/12)(1-\nu^2)^{-5/8}E(h/a)^{5/4}(a/L)^{1/2} \qquad \text{(A-15a)}$$

for $10(h/a)^{1/2} < L/a < 3(a/h)^{1/2}$

$$\tau_{cr} = 0.272\ (1-\nu^2)^{-3/4}E(h/a)^{3/2} \qquad \text{(A-15b)}$$

for $L/a > 3(a/h)^{1/2}$

Appendix B

COMPUTER PROGRAM LISTING AND DESCRIPTION

The first harmonic field in the field winding for a two pole (p=1) machine is given by (Table 1).

$$B_{rfw} = \frac{2\mu_o J_f \sin\left(\frac{\theta_{wfe}}{2}\right)\sin(\theta-\phi)}{3\pi} r\left[-2-\left(\frac{R_{fi}}{r}\right)^3+3\left(\frac{r}{R_{fo}}\right)^{-1}+\left(\frac{r}{R_s}\right)^{-1}\left(\frac{R_{fo}}{R_s}\right)^3(1-y^3)\right] \qquad \text{(A-16)}$$

The maximum flux density in the r direction can be found by taking the derivative of B_{rfw} with respect to r and setting it equal to zero, which gives a simple result for a two pole machine

$$r = R_{fi} \qquad \text{(A-17)}$$

and the maximum flux density in the field winding is

$$B_{max} = \frac{2\mu_o J_f \sin\left(\frac{\theta_{wfe}}{2}\right)R_{fo}}{3\pi}\left[-3y+3+\left(\frac{R_{fo}}{R_s}\right)^2(1-y^3)\right] \qquad \text{(A-18)}$$

This linear relation between B_{max} and J_f defines the magnet line which was shown in Figs. 8 and 7. If an operating point is chosen (given B_{max} and J_f) and field winding inside and outside radiuses are specified, equation (A-18) can be solved for R_s, shield inside radius. Although fields generated by the armature phases try to oppose the fields generated by field winding thus reducing B_{max}, there will be additional field concentration due to armature end turns and higher space harmonics. Thus, calculating B_{max} by equation (A-18) is a conservative assumption.

After the location of the iron shield is fixed, the first thing to be checked is the saturation limitations. Fig. A-2 shows the flux linkages through the iron shield. The total flux carried by the shield, for a two pole machine

$$\Phi_{A-A} = \int_0^{\pi/2} B_{rfo}\,(R_s)\; \ell_s\; R_s\; d\theta \qquad \text{(A-19)}$$

where the first harmonic component of B_{rfo} comes from Table 1 and is given by

$$B_{rfo} = \frac{2J_f \sin\left(\frac{\theta_{wfe}}{2}\right)\cos\theta}{3\pi}\, r\left(\frac{R_{fo}}{r}\right)^3 (1-y^3)\left[1+\left(\frac{r}{R_s}\right)^2\right] \qquad \text{(A-20)}$$

When equation (A-20) is evaluated at $r = R_s$ and substituted into (A-19), integration gives

$$\Phi_{A-A} = \frac{4\mu_o\, J_f \sin\left(\frac{\theta_{wfe}}{2}\right)}{3\pi}\, \frac{R_{fo}^3}{R_s}\, \ell_s (1-y^3) \qquad \text{(A-21)}$$

The limitations on saturation require that

$$\Phi_{A-A} \leq B_{sat}\,(R_{os}-R_s)\; \ell_s \qquad \text{(A-22)}$$

When equations (A-21) and (A-22) are combined, the minimum shield outside radius, R_{os} is

$$R_{os} = \frac{4\mu_o\, J_f \sin\left(\frac{\theta_{wfe}}{2}\right)}{3\pi\, B_{sat}}\, \frac{R_{fo}^3}{R_s}(1-y^3) + R_s \qquad \text{(A-23)}$$

where B_{sat} is the saturation flux density of the iron shield. $B_{sat} = 1.5$ Weber/m^2 was used in the program.

Local saturation of the iron shield requires that

$$B_{rfo}(R_s) = \frac{4\mu_o\, J_f \sin\left(\frac{\theta_{wfe}}{2}\right)}{3\pi} R_s \left(\frac{R_{fo}}{R_s}\right)^3 (1-y^3) \leq B_{sat} \qquad \text{(A-24)}$$

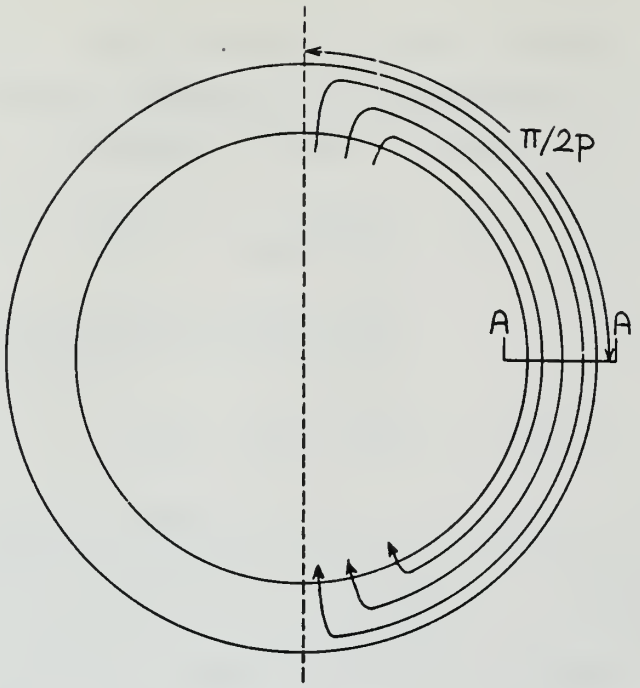

Figure A-2
Flux Pattern in Iron Shield

Algebraic manipulation of equation (A-23) and (A-24) gives

$$R_{os} - R_s \leqslant R_s \qquad \text{(A-25)}$$

This is to say that shield thickness must be less than or equal to shield inside radius. Since R_s is fixed from equation (A-18), calculated R_{os} may not satisfy this condition. In this case, program rejects this particular design and prints a message saying "NO SOLUTION". Same message is also printed when equation (A-18) gives R_s less than R_{fo}.

The maximum airgap length can be found by assuming that armature inside and outside radiuses coincide, that is

$$\Delta_{max} = R_s - t - R_{fo} \qquad \text{(A-26)}$$

where t is the radial distance between shield inside radius and armature end turns. In the program, this Δ_{max} is

divided into n steps (n=50 in this program) and in each iteration airgap length Δ is incremented by $\Delta_{max}/50$.

Given Δ, armature inside radius R_{ai}

$$R_{ai} = R_{fo} + \Delta \qquad \text{(A-27)}$$

and armature outside radius, R_{ao}

$$R_{ao} = (R_s + R_{ai} - t)/2.0 \qquad \text{(A-28)}$$

The program then proceeds to sum up the infinite series given in Table A-2 of Chapter 2 for $L_a - L_{ab}$. Then synchronous reactance is normalized to internal voltage and x_a as given by equation(6)is calculated. Table A-2 gives the effective lengths used in this study[16]. Equation 7 is then utilized to give an expression for the straight section length, which results in a second degree equation for the straight section length. This equation is too complicated to write explicitly and will be omitted here. Total machine length is given by

$$\ell_t = \ell + 2\Delta\ell \qquad \text{(A-29)}$$

After all machine dimensions are calculated, the program then proceeds to calculate machine reactances. Synchronous reactance x_d given by(9),transient reactance x_d' given by(8)can be calculated by summing the series. It should be pointed out that up to 15 harmonics were used. The user is free to choose number of harmonics to be summed.

To calculate subtransient reactance x_d'' , the primary shield radius has to be specified. Since for a given airgap length, the range of R_t is known and this can be done easily by incrementing R_t in each iteration. For a previously calculated airgap length Δ, R_t is
(m=50 used in this study) $R_t = R_{fo} + \frac{\Delta}{m}$ (A-30)

TABLE A-2

Effective Lengths

Armature end turn length	$\Delta\ell = R_{ai} + R_{ao}$
Effective lengths: armature self inductance	$\ell_a = \ell + \Delta\ell$
Mutual inductance, field-to-armature	$\ell_m = \ell$
Mutual inductance, field-to-damper	$\ell_{fd} = \ell$
Eddy-current loss	$\ell_{ed} = \ell$
Conduction loss	$\ell_c = \ell + 2\Delta\ell$
Field winding end turn length	$\Delta\ell_f = R_{fo} + R_{fi}$

Then x_d'' can be calculated from(10).

Next step is to calculate required primary shield thickness, to give time constant such that, field current rise will not be higher than the specified value (SUBROUTINE TIC). Since the maximum field current rise will be from 25

$$i_{f_{max}} = i_{fo}\left[1 + \frac{x_d - x_d'}{x_d'}\right] \qquad (A\text{-}31)$$

which depends on $\frac{x_d - x_d'}{x_d'}$. If the maximum rise is less than the specified rise, then the required shield thickness or time constant is set to zero. This is to say that the primary shield will be a very thin highly conductive layer where induced currents flow. In this study, it was assumed that the time constant of shield structure is zero.

Having specified primary shield thickness, the radial stresses σ_o under three-phase fault from load is calculated (SUBROUTINE STRES) by(21).

The most important section of the program is SUBROUTINE SHIEL which designs the shield structure according to the given working stresses. The designed shield must satisfy the following conditions:

1) $$w_1 + h_h + h + w_2 = \Delta$$

where h_h is the primary shield thickness, h is the shield structure thickness and w_1 and w_2 are the deflections in two directions.

2) $$R_t - h_h - h/2 = a$$ -if primary shield is outside the shield structure

$$R_t + h/2 = a$$ -if primary shield is inside shield structure

3) $S_c \leq W_{sic}$

$S_t \leq W_{sit}$

$S_s \leq W_{sis}$

where S_c, S_t, S_s are induced stresses in compression, tension and shear respectively and W_{sic}, W_{sit}, W_{sis} are the working stresses in compression, tension, and shear respectively.

4) $(\tau_{x\theta})_{max} \leq W_{sis}$ stresses induced under line-to-line short circuit from load

$\tau_{cr} \geq (\tau_{x\theta})_{max}$

A total of 8 principal stresses are calculated after W_1 and W_2 are found by equation (A-4). These are at $\theta=0$ and $\theta=\pi/2$, on the top and bottom surface. All of the stresses mentioned above are at the midlength where maximum stresses occur. Shield length was assumed to cover straight section length plus field winding end turns. After checking each of them by the requirements specified above, the progrm proceeds to check on requirement 4. If, in the course of these calculations, any one of the requirements is not satisfied, computations are repeated by incrementing shield structure thickness, until specified airgap is filled with shield structure. Figure A-3 shows the region to be scanned by the program. Since the smallest airgap length will give minimum weight or volume machine, the solution will return to the main program if all four of the requirements are satisfied. There may be other solutions at bigger airgap lengths which we will not investigate.

Machine volume is calculated by

$$V = \pi R_{os}^2 . \ell_t$$

and machine weight by

$$W=\pi(R_{ao}^2-R_{ai}^2).\ell.\rho_a+\pi(R_{os}^2-R_s^2)\ell_t\cdot\rho_s+\pi(R_{fo}^2-R_{fi}^2)\ell_t\cdot\rho_f$$

$$+8\pi.\Delta\ell(R_{ao}^2-R_{ao}.R_{ai})\rho_{et}+\pi(R_{so}^2-R_{si}^2)\ell_{ss}\cdot\rho_{ss}$$

where

ρ_a - armature density = 4500 Kg/m^3

ρ_s - iron shield density = 8000 Kg/m^3

ρ_f - rotor density = 4500 Kg/m^3

ρ_{et} - end turns density = 4000 Kg/m^3

ρ_{ss} - shield structure density = depends on program input

These average densities are used in the program.
For selected values of n, m and increment of h, the shield structure thickness solution may not converge or may converge at a longer airgap length, if these values are small. Smaller step sizes will increase computation time and give true convergence, so some sort of a comprimise should be done. If the solution does not converge then program prints a message saying "NO CONVERGENCE".

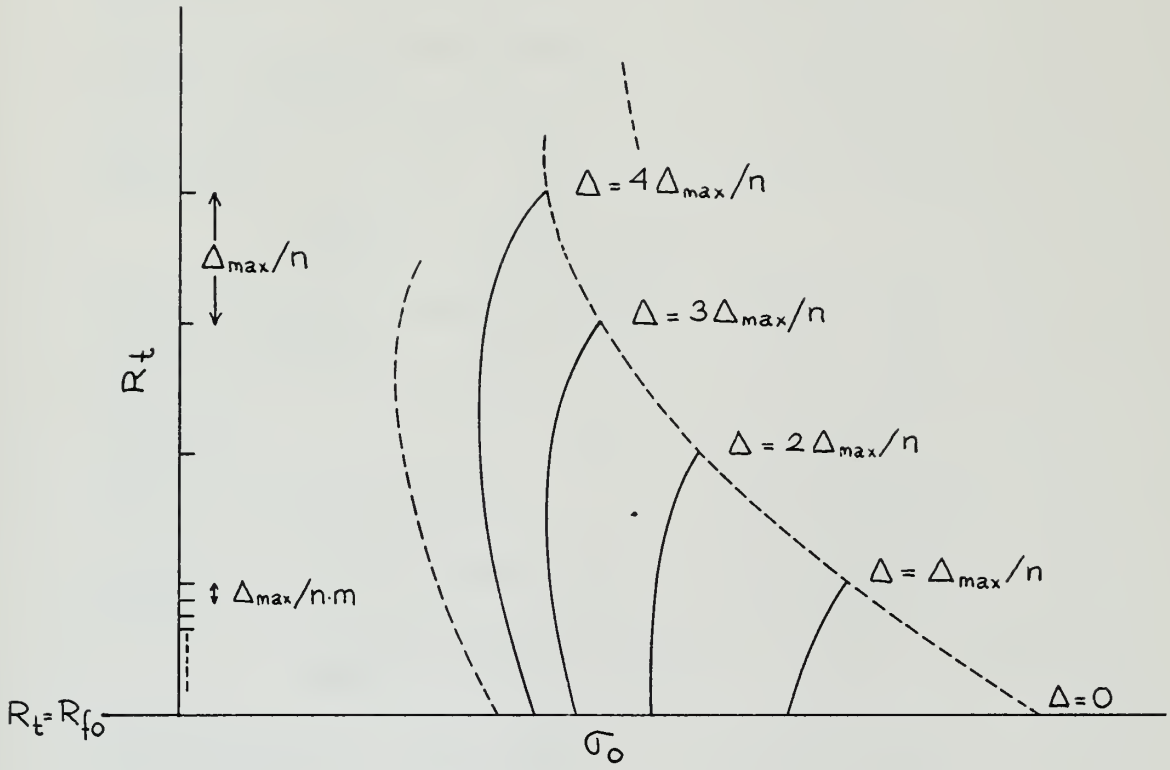

Figure A-3
Region Scanned by the Program

Main program and subroutines are listed in Tables A-3, A-4, A-5, and A-6. Table A-6 gives the sample program input which is described below.

Card 1 Format 3F10.2

Horsepower Rating	col. 1-10
Power Factor	col.11-20
Design RPM	col.21-30

Card 2 Format 2F10.2

Field winding outside radius, inches	col. 1-10
Field winding inside radius, inches	col.11-20

Card 3. Format 3F10.2

Maximum flux density in field winding, Tesla	col. 1-10
Rated field current density $\times 10^{-8}$, amp/m^2	col. 11-20
Field winding angle, θ_{wf} degrees	col. 21-30

Card 4 Format 4F10.2

Rated armature current density $\times 10^{-6}$, amp/m^2	col. 1-10
Armature winding angle, θ_{wa}, degrees	col. 11-20
Armature space factor	col. 21-30
Armature filament diameter, inches	col. 31-40

Card 5 Format 7F10.2

Shield structure material young modulus $\times 10^{-6}$, psi	col. 1-10
Shield structure material poisson ratio	col. 11-20
Primary shield conductivity $\times 10^{-7}$, mho/m	col. 21-30
Shield structure density, lbs/in^3	col. 31-40
Working stresses in tension, psi	col. 41-50
Working stresses in compression, psi	col. 51-60
Working stresses in shear, psi	col. 61-70

Card 6 Format 3F10.2

Circuit breaker opening time, cycles	col. 1-10
Rated field current, amp	col. 11-20
Allowable field current rise,amp	col. 21-30

Card 7

Format I1, if 1 is punched in column one, program makes calculation for the case where primary shield is under shield structure; and, if 2 is punched, calculations are performed for the case where primary shield is on the shield structure.

Format F10.2, distance between shield inside radius and armature end turns, inches col. 11-20.

TABLE A-3

Main Program

```
// DENIZMEN,CLASS=C,REGION=120K
/*MITID USER=(M10615,8923,,,EVRENLIN)
/*SRI LOW
/*MAIN TIME=3
/*FORMAT PR,DDNAME=FT06F001,FORMS=THESIS
//TESTRUN EXEC FORCGO
//C.SYSIN  DD  *,DCB=BLKSIZE=2000
      IMPLICIT REAL*8 (A-H,O-Z)
      DIMENSION SSS(8),SS(8)
      READ(5,100) P,PF,RPM
      READ(5,200) RFOI,RFII
      READ(5,100) BMAX,FII,TWF
      READ(5,300) AJJ,TWA,ASF,DW
      READ(5,400) YMM,UN,SCC,GM,WSIT,WSIC,WSIS
      READ(5,100) CBOI,RFC,DFC
      READ(5,500) KK,T
  100 FORMAT(3F10.2)
  200 FORMAT(2F10.2)
  300 FORMAT(4F10.2)
  400 FORMAT(7F10.2)
  500 FORMAT(I1,9X,F10.1)
      FI=FII*1.0D08
      AJ=AJJ*1.0D06
      YM=YMM*1.0D06
      SC=SCC*1.0D07
      W=0.10471975500*RPM
      RTWF=TWF*0.01745329200
      RTWA=TWA*0.01745329200
      VA=P/(PF*1.341D-03)
      VAA=VA/1.0D06
      PFS=DSQRT(1.0D0-PF**2)
      WRITE(6,600)
  600 FORMAT('1','DESIGN CONSTANTS')
      WRITE(6,601) P
  601 FORMAT('0','DESIGN HORSEPOWER=',F10.2)
```

```
      WRITE(6,602) VAA
  602 FORMAT('0','MVA RATING=',F7.2)
      WRITE(6,603) PF
  603 FORMAT('0','POWER FACTOR=',F4.2)
      WRITE(6,604) RPM
  604 FORMAT('0','DESIGN RPM=',F6.1)
      WRITE(6,605) FII
  605 FORMAT('0','RATED FIELD CURRENT DENSITY=',F4.2,3X,'10 8 A/M2')
      WRITE(6,606) AJJ
  606 FORMAT('0','RATED ARMATURE CURRENT DENSITY=',F4.2,3X,'10 6 A/M2')
      WRITE(6,607) BMAX
  607 FORMAT('0','MAXIMUM FLUX DENSITY IN FIELD WINDING=',F4.2,3X,'TESLA
     1S')
      WRITE(6,608) TWF
  608 FORMAT('0','FIELD WINDING ANGLE=',F6.2,3X,'DEG.')
      WRITE(6,609) TWA
  609 FORMAT('0','ARMATURE WINDING ANGLE=',F6.2,3X,'DEG.')
      WRITE(6,610) ASF
  610 FORMAT('0','ARMATURE SPACE FACTOR=',F4.2)
      WRITE(6,611) DW
  611 FORMAT('0','ARMATURE FILAMENT DIAMETER=',F5.3,3X,'IN.')
      WRITE(6,612) YMM
  612 FORMAT('0','YOUNG MODULUS OF SHIELD SUPPORT MATERIAL=',F4.1,3X,'10
     1 6 PSI.')
      WRITE(6,613) UN
  613 FORMAT('0','POISSON RATIO OF SHIELD SUPPORT MATERIAL=',F5.3)
      WRITE(6,614) SCC
  614 FORMAT('0','ELECTRICAL CONDUCTIVITY OF SHIELD=',F3.1,3X,'10 7 MHO/
     1M')
      WRITE(6,615) GM
  615 FORMAT('0','DENSITY OF SHIELD SUPPORT MATERIAL=',F5.3,3X,'LBS/IN3'
     1)
      WRITE(6,616) WSIT
  616 FORMAT('0','WORKING STRESS IN TENSION=',F7.1,3X,'PSI.')
      WRITE(6,617) WSIC
```

```
617 FORMAT('0','WORKING STRESS IN COMPRESSION=',F7.1,3X,'PSI.')
    WRITE(6,618) WSIS
618 FORMAT('0','WORKING STRESS IN SHEAR=',F7.1,3X,'PSI.')
    WRITE(6,619) CBOT
619 FORMAT('0','CIRCUIT BREAKER OPENNING TIME=',F4.1,3X,'CYCLES')
    WRITE(6,620) RFC
620 FORMAT('0','RATED FIELD CURRENT=',F6.1,3X,'AMP.')
    WRITE(6,621) DFC
621 FORMAT('0','ALLOWABLE FIELD CURRENT RISE=',F6.1,3X,'AMP.')
    RFO=RFOI*0.0254D0
    RFI=RFII*0.0254D0
    Y=RFI/RFO
    A1=3.0*BMAX/(2.0*(4.0D-07)*FI*DSIN(RTWF/2.0)*RFO)
    A2=A1+3.0*Y-3.0
    IF(A2.LE.0.0D0) GO TO 15
    A3=DSQRT(A2/(1.0-Y**3))
    RS=RFO/A3
    A4=4.0*(4.0D-07)*FI*DSIN(RTWF/2.0)/(3.0*1.5)
    ROS=A4*(RFO**3)*(1.0-Y**3)/RS+RS
    A5=ROS-RS
    IF(A5.GT.RS) GO TO 15
    RAOM=RS-T*0.0254D0
    DELM=RAOM-RFO
    DELMM=DELM/50.0D0
    DO 717 NN=1,49
    DEL=NN*DELMM
    DELA=DEL/50.0D0
    RAI=RFO+DEL
    RAO=(RS+RAI-T*0.0254D0)/2.0D0
    X=RAI/RAO
    CIP=(1.0-X+(1.0-X**3)*((RAO/RS)**2)/3.0)/3.0
    SUM=0.0
    DO 30 I=1,15,2
    S=DFLOAT(I)
    CSNP=(2.0-S-4.0*(X**(S+2.0))+(S+2.0)*(X**4)+2.0*(2.0-S)*((1.0-X**(
   1S+2.0))**2)*((RAO/RS)**(2.0*S))/(2.0+S))/(S*(4.0-S**2))
    CP=(((DSIN(S*RTWA/2.0))**2)*(1.0-DCOS(2.0*S*3.141592653/3.0)))/(S*
   1*2)
```

```
      CPP=CP*CSNP
      SUM=SUM+CPP
   30 CONTINUE
      XAP=(AJ*((RAO/RFO)**3)*SUM)/(DSQRT(2.0D0)*FI*(DSIN(RTWA/2.0))*(DSI
     1N(RTWF/2.0))*(1.0-Y**3)*C1P)
      A6=1.0-XAP**2
      IF(A6.LE.0.0D0) GO TO 717
      A7=24.0*W*4.0*(3.141592653D-07)*FI*AJ*(1.0-Y**3)*(RFO**3)*RAO*(DSI9
     1N(RTWA/2.0))*(DSIN(RTWF/2.0))*C1P/(3.141592653*DSQRT(2.0D0))
      A8=VA/A7
      DELL=RAO+RAI
      C=2.0*A8*XAP*PFS+2.0*DELL*XAP**2
      D=(A8**2)+2.0*A8*DELL*XAP*PFS+(DELL*XAP)**2
      SL=(C+DSQRT(4.0*A6*D+C**2))/(2.0*A6)
      SLT=SL+2.0*DELL
      SL1=SL+2.0*(RFO+RFI)
      XA=XAP*(SL+DELL)/SL
      A10=1.0-(XA*PF)**2
      IF(A10.LT.0.0D0) GO TO 717
      XD=XA/(DSQRT(A10)-XA*PFS)
      A11=16.0*SL*(4.0D-07)/((1.0-Y**2)**2)
      SUM1=0.0
      DO 40 I=1,15,2
      S=DFLOAT(I)
      FL1=((DSIN(S*RTWF/2.0))**2)/((S**2-4.0)*S**3)
      FL2=S-2.0+4.0*Y**(S+2.0)-(S+2.0)*Y**4+2.0*(S-2.0)*((1.0-Y**(S+2.0)
     1)**2)*((RFO/RS)**(2.0*S))/(S+2.0)
      SUM1=SUM1+FL1*FL2
   40 CONTINUE
      SUM1=SUM1*A11
      SUM2=SUM*16.0*(SL+DELL)*(4.0D-07)/((1.0-X**2)**2)
      A12=(1.0-X+(1.0-X**3)*((RAO/RS)**2)/3.0)/3.0
      A13=(1.0-Y**2)*(1.0-X**2)
      A14=32.0*SL*(4.0D-07)*(DSIN(RTWA/2.0))*(DSIN(RTWF/2.0))*(1.0-Y**3)
     1*(RFO/RAO)*A12/A13
```

```
      A15=A14**2
      XDP=XD*(1.0-1.5*A15/(SUM2*SUM1))
      DO 718 KN=1,49
      RT=RFO+KN*DELA
      A16=4.0*(3.141592653D-07)*SL*3.141592653*(1.0+(RT/RS)**2)/8.0
      A17=1.0-X+(1.0-X**3)*((RAO/RS)**2)/3.0
      A18=8.0*(3.141592653D-07)*SL*(DSIN(RTWA/2.0))*(RT/RAO)*A17/(1.0-X*
     1*2)
      A19=A18**2
      XDPP=XD*(1.0-1.5*A19/(SUM2*A16))
      A100=DFC/RFC
      A101=(XD-XDP)/XDP
      IF(A101.LT.A100) GO TO 99
      CALL TIC(XD,XDP,XDPP,CBOT,RT,RS,SC,HH,W,A100,A101)
      GO TO 98
   99 HH=0.0D0
   98 CALL STRES(RT,RS,FI,RTWF,RFO,Y,XDPP,RTWA,AJ,RAO,RO,PFS,PF,X,VBSR)
      CALL SHIEL(YM,UN,W,RO,GM,HH,KK,RFO,RAI,H,SL1,W11,W22,VBSR,XDPP,VA,
     1TMAX,WSIT,WSIC,WSIS,RT,NS,DEL,A)
      IF(NS.EQ.0) GO TO 718
      IF(NS.EQ.1) GO TO 11
  718 CONTINUE
      GO TO 717
   11 GO TO 777
  717 CONTINUE
      WRITE(6,930)
  930 FORMAT('1','NO CONVERGENCE')
      GO TO 17
  777 VOL=3.141592653D0*(ROS**2)*SLT
      W1=3.141592653*SL*4500.0*(RAO**2-RAI**2)
      W2=3.141592653*SLT*8000.0*(ROS**2-RS**2)
      W3=3.141592653*SLT*4500.0*(RFO**2-RFI**2)
      W4=3.141592653*DELL*4000.0*8.0*(RAO**2-RAO*RAI)
      ARO=A+H/2.0D0
      ARI=A-H/2.0D0
```

```
      W6=3.14159265D0*(ARO**2-ARI**2)*SL1*39.3700787D0*GM
      W5=W1+W2+W3+W4
      PCC=3.0*RTWA*(AJ**2)*(RAO**2)*(1.0-X**2)*SLT/(ASF*6.0D07)
      BAV1=1.0/(RAO-RAI)
      BAV2=(2.0*(4.0D-07)*FI*(RFO**3)*(DSIN(RTWF/2.0))*(1.0-Y**3)/3.0)**
     12
      BAV3=(1.0-X**3)/(3.0*RAI**3)+(1.0-X)*((2.0/RAI)+RAO/(RS**2))/(RS**
     12)
      BAVS=BAV1*BAV2*BAV3
      PEC=3.0*RTWA*(RAO**2)*(1.0-X**2)*(W**2)*(6.0D07)*ASF*BAVS*SL*((DW*
     10.0254)**2)/32.0
      PSH=3.141592653*((ROS**2)-(RS**2))*SLT*1.85*(8.0D06)/453.0
      PPD=(PCC+PEC+PSH)*100.0/VA
      CI=100.0/2.54
      RAII=RAI*CI
      RAOI=RAO*CI
      RSI=RS*CI
      ROSI=ROS*CI
      SLTI=SLT*CI
      SL=SL*CI
      VOLI=VOL/0.028317
      WSI=W5*2.204623D0+W6
      HH=HH*CI
      DEL=DEL*CI
      RT=RT*CI
      WRITE(6,900) RFOI
  900 FORMAT('1','FIELD WINDING OUTSIDE RADIUS=',F7.3,3X,'IN.')
      WRITE(6,901) RFII
  901 FORMAT('0','FIELD WINDING INSIDE RADIUS=',F7.3,3X,'IN.')
      WRITE(6,902) RAII
  902 FORMAT('0','ARMATURE INSIDE RADIUS=',F7.3,3X,'IN.')
      WRITE(6,903) RAOI
  903 FORMAT('0','ARMATURE OUTSIDE RADIUS=',F7.3,3X,'IN.')
      WRITE(6,904) RSI
  904 FORMAT('0','SHIELD INSIDE RADIUS=',F7.3,3X,'IN.')
```

```
      WRITE(6,905) ROSI
  905 FORMAT('0','SHIELD OUTSIDE RADIUS=',F7.3,3X,'IN.')
      WRITE(6,906) SLTI
  906 FORMAT('0','TOTAL LENGTH=',F7.3,3X,'IN.')
      WRITE(6,907) SL
  907 FORMAT('0','STRAIGHT SECTION LENGTH=',F7.3,3X,'IN.')
      WRITE(6,908) VOLI
  908 FORMAT('0','MACHINE VOLUME=',F9.3,3X,'FT 3')
      WRITE(6,909) WSI
  909 FORMAT('0','WEIGHT OF ACTIVE PARTS=',F10.3,3X,'LBS.')
      IF(KK.EQ.2) GO TO 817
      WRITE(6,951)
  951 FORMAT('0','PRIMARY SHIELD IS UNDER THE SHIELD STRUCTURE')
      GO TO 818
  817 WRITE(6,931)
  931 FORMAT('0','PRIMARY SHIELD IS ON THE SHIELD STRUCTURE')
  818 WRITE(6,914) DEL
  914 FORMAT('0','AIR GAP LENGTH=',F7.4,3X,'IN.')
      WRITE(6,921) RT
  921 FORMAT('0','PRIMARY SHIELD OUTSIDE RADIUS=',F7.3,3X,'IN.')
      WRITE(6,941) ARO
  941 FORMAT('0','SHIELD STRUCTURE OUTSIDE RADIUS=',F7.4,3X,'IN.')
      WRITE(6,910) HH
  910 FORMAT('0','PRIMARY SHIELD THICKNESS=',F7.4,3X,'IN.')
      WRITE(6,911) H
  911 FORMAT('0','SHIELD STRUCTURE THICKNESS=',F7.4,3X,'IN.')
      WRITE(6,912) W11
  912 FORMAT('0','SHIELD DEFLECTION TOWARDS FIELD WINDING UNDER THREE PH
     1ASE FAULT=',F7.4,3X,'IN.')
      WRITE(6,913) W22
  913 FORMAT('0','SHIELD DEFLECTION TOWARDS ARMATURE WINDING UNDER9THREE
     1 PHASE FAULT=',F7.4,3X,'IN.')
      WRITE(6,916) XD
  916 FORMAT('0','SYNCHRONOUS REACTANCE P.U.=',F6.4)
      WRITE(6,917) XDP
```

```
  917 FORMAT('0','TRANSIENT REACTANCE P.U.=',F6.4)
      WRITE(6,918) XDPP
  918 FORMAT('0','SUBTRANSIENT REACTANCE P.U.=',F6.4)
      WRITE(6,919) PPD
  919 FORMAT('0','MACHINE LOSSES PERCENT OF MACHINE RATING=',F5.3)
      WRITE(6,915) RO
  915 FORMAT('0','MAX. RADIAL STRESS UNDER THREE PHASE FAULT=',F8.1,3X,'
     1PSI.')
      WRITE(6,920) TMAX
  920 FORMAT('0','MAXIMUM TORQUE UNDER LINE TO LINE SHORT CIRCUIT FROM L
     1OAD P.U.=',F7.3)
      GO TO 17
   15 WRITE(6,800)
  800 FORMAT('1','NO SOLUTION')
   17 STOP
      END
```

TABLE A-4

Subroutine Tic

```
SUBROUTINE TIC(XD,XDP,XDPP,CBOT,RT,RS,SC,HH,W,A100,A101)
IMPLICIT REAL*8 (A-H,O-Z)
A=DLOG(1.0D0-A100/A101)
B=2.0D0*3.141592653D0*CBOT/W
C=(XDPP/XDP)*((XDP-XDPP)/(XD-XDPP))
D=SC*4.0D0*3.141592653D0*1.0D-07*RT*(1.0D0+(RT/RS)**2)/2.0D0
HH=B/(A*C*D)
RETURN
END
```

TABLE A-5

Subroutine Stres

```
      SUBROUTINE STRES(RT,RS,FI,RTWF,RFO,Y,XDPP,RTWA,AJ,RAO,RO,PFS,PF,X,
     1VBSR)
      IMPLICIT REAL*8 (A-H,O-Z)
      F1=(RT/RS)**2
      F=(1.0D0-F1)/(1.0D0+F1)
      HFT1=2.0D0*FI*DSIN(RTWF/2.0D0)*RT*((RFO/RT)**3)*(1.0D0-Y**3)/(3.0D
     10*3.14159265300)
      HFT=HFT1*(1.0D0-F1)
      VBSR=DSQRT((1.0D0+XDPP*PFS)**2+(XDPP*PF)**2)
      HA1=1.0D0-X+(((RAO/RS)**2)/3.0D0)*(1.0D0-X**3)
      HA=HA1*1.350474474D0*AJ*(VBSR/XDPP)*DSIN(RTWA/2.0D0)*RT*(RAO/RT)
      RO=(8.0D0*3.141592653D-07*HA*(1.0D0+F)*(HA*(1.0D0+F)+HFT))*1.45161
     1D-04
      RETURN
      END
```

TABLE A-6

Subroutine Shiel

```
      SUBROUTINE SHIEL(YM,UN,W,RO,GM,HH,KK,RFO,RAI,H,SL1,W11,W22,VBSR,XD
     1PP,VA,TMAX,WSIT,WSIC,WSIS,RT,NS,DEL,A)
      IMPLICIT REAL*8 (A-H,O-Z)
      DIMENSION SSS(8),SS(8)
      DO 10 KM=1,10000
      H=0.001D0*DFLOAT(KM)
      IF(KK.EQ.1) GO TO 5
      A=(RT-HH)*39.3700787 4D0-H/2.0D0
      ANA=(A-H/2.0D0)*0.0254D0
      IF(ANA.GT.RFO) GO TO 6
      NS=0
      RETURN
    5 A=R1*39.37007874D0+H/2.0D0
      ANA=(A+H/2.0D0)*0.0254D0
      IF(ANA.LT.RAI) GO TO 6
      NS=0
      RETURN
    6 A1=1.0D0-UN**2
      A2=3.141592653D0
      A3=A2**2
      A20=YM/A1
      PL=SL1*39.3700787 4D0
      P=GM*(W**2)*A*H/386.4D0
      D=YM*(H**3)/(A1*12.0D0)
      BET=(3.0D0*A1/(A*H)**2)**0.25
      ALP=BET*PL/2.0D0
      A4=PL/A
      A5=A4**2
      A6=H/(2.0D0*PL)
      A7=A6**2
      A8=(PL**4)*A7*RO/(2.0D0*D)
```

```
      C0=A8/(3.0D0*A5*A1+A7*A3**2)
      AAF=2.0D0*A3+(1.0D0-UN)*4.0D0*A5
      AAG=(1.0D0+UN)*A4*A2*2.0D0
      AAK=UN*A4*A2*2.0D0
      AAL=(1.0D0+UN)*A2*A4*6.0D0
      AAM=(1.0D0-UN)*A3*3.0D0+A5*24.0D0
      AAN=A5*12.0D0
      AAP=UN*A2*A4*3.0D0
      AAR=A5*(3.0D0+A7*((2.0D0-UN)*A3+A5*4.0D0))*2.0D0
      AAS=A5*3.0D0+A7*(A3+A5*4.0D0)**2
      A9=AAS*AAG/AAK-AAR
      A10=AAN*AAG/AAK-AAM
      A11=AAP-AAF*AAS/AAK
      A12=AAL-AAN*AAF/AAK
      A0=-UN*A4*C0/A2
      V=A9-A10*A11/A12
      B2=A8/V
      A22=-B2*A10/A12
      C2=(B2*AAG-A22*AAF)/AAK
      A13=P*(PL**4)/(64.0D0*D*ALP**4)
      IF(ALP.GT.85.0D0) GO TO 8
      ADP=(DCOS(ALP))*(DCOSH(ALP))*2.0D0/(DCOS(2.0D0*ALP)+DCOSH(2.0D0*AL
     1P))
      AFP=(DSIN(ALP))*(DSINH(ALP))*2.0D0/(DCOS(2.0D0*ALP)+DCOSH(2.0D0*AL
     1P))
      GO TO 9
    8 ADP=0.0D0
      AFP=0.0D0
    9 W1=C0+C2-(1.0D0-ADP)*A13
      W2=C0-C2-(1.0D0-ADP)*A13
      W11=W1
      W22=W2
      IF(W1.LT.0.0D0) GO TO 50
      IF(W2.LT.0.0D0) GO TO 51
      IF(W1.GT.W2) GO TO 54
```

```
      WW=W2
      W1=W2
      W2=0.0D0
      GO TO 53
   54 WW=W1
      W2=0.0D0
      W1=W1
      GO TO 53
   51 WW=W1-W2
      W2=-W2
      W1=W1
      GO TO 53
   50 IF(W2.LT.0.0D0) GO TO 52
      W100=W2
      WW=W2-W1
      W2=-W1
      W1=W100
      GO TO 53
   52 W10=DABS(W1)
      W20=DABS(W2)
      IF(W10.GT.W20) GO TO 55
      WW=-W2
      W2=-W2
      W1=0.0D0
      GO TO 53
   55 WW=-W1
      W2=-W1
      W1=0.0D0
   53 HO=WW+H+HH*39.37007874D0
      HO1=DABS(HO-DEL*39.37007874D0)
      IF(HO1.LE.0.08D0) GO TO 21
      GO TO 10
   21 IF(KK.EQ.1) GO TO 22
      ABA=RT*39.37007874D0+W2
      ABA1=DABS(RAI*39.37007874D0-ABA)
```

```
      IF(ABA1.LE.0.08D0) GO TO 23
      GO TO 10
   22 ABA=(RT-HH)*39.37007874D0-W1
      ABA1=DABS(RF0*39.37007874D0-ABA)
      IF(ABA1.LE.0.08D0) GO TO 23
      GO TO 10
   23 EX01=-A2*(A0+A22)/PL-UN*A13*(1.0D0-ADP)/A
      EX02=-A2*(A0-A22)/PL-UN*A13*(1.0D0-ADP)/A
      ET01=2.0D0*B2/A-(C0+C2-A13*(1.0D0-ADP))/A
      ET02=-2.0D0*B2/A-(C0-C2-A13*(1.0D0-ADP))/A
      XT1=2.0D0*(B2-2.0D0*C2)/(A**2)
      XT2=-2.0D0*(B2-2.0D0*C2)/(A**2)
      XX1=-A3*(C0+C2)/(PL**2)+2.0D0*A13*(BET**2)*AFP
      XX2=-A3*(C0-C2)/(PL**2)+2.0D0*A13*(BET**2)*AFP
      SSS(1)=A20*(EX01+UN*ET01+H*(XX1+UN*XT1)/2.0D0)
      SSS(3)=A20*(EX02+UN*ET02+H*(XX2+UN*XT2)/2.0D0)
      SSS(5)=A20*(EX01+UN*ET01-H*(XX1+UN*XT1)/2.0D0)
      SSS(7)=A20*(EX02+UN*ET02-H*(XX2+UN*XT2)/2.0D0)
      SSS(2)=A20*(ET01+UN*EX01+H*(XT1+UN*XX1)/2.0D0)
      SSS(6)=A20*(ET01+UN*EX01-H*(XT1+UN*XX1)/2.0D0)
      SSS(4)=A20*(ET02+UN*EX02+H*(XT2+UN*XX2)/2.0D0)
      SSS(8)=A20*(ET02+UN*EX02-H*(XT2+UN*XX2)/2.0D0)
      DO 20 I=1,8
      IF(SSS(I).LT.0.0D0) GO TO 41
      IF(SSS(I).GE.WSIT) GO TO 10
      GO TO 20
   41 DSEN=DABS(SSS(I))
      IF(DSEN.GE.WSIC) GO TO 10
   20 CONTINUE
      DO 30 I=1,7,2
      SS(I)=(SSS(I)-SSS(I+1))/2.0D0
   30 CONTINUE
      DO 40 I=1,7,2
      A112=DABS(SS(I))
      IF(A112.GE.WSIS) GO TO 10
   40 CONTINUE
```

```
      TRAT=(VA*0.738D0/W)*12.0D0
      TMAX=1.3D0*TRAT*(VBSR**2)/XDPP
      ROX=GM*(W**2)*(A**2)/386.4D0
      SST=2.0D0*TMAX*(A+H/2.0D0)
      SSA=3.14159265D0*((A+H/2.0D0)**4-(A-H/2.0D0)**4)
      SSB=SST/SSA
      TTT=2.0D0*DSQRT((ROX/2.0D0)**2+SSB**2)
      IF(TTT.GT.WSIS) GO TO 10
      A300=3.0D0*DSQRT(A/H)
      A301=PL/A
      IF(A301.GT.A300) GO TO 71
      TCR=0.699096978D0*YM*((H/A)**(5.0D0/4.0D0))*(DSQRT(A/PL))/((1.0D0-
     1UN**2)**(5.0D0/8.0D0))
      GO TO 72
   71 TCR=0.272D0*YM*((H/A)**1.5)/((1.0D0-UN**2)**0.75D0)
   72 IF(TCR.LT.TTT) GO TO 10
      TMAX=TMAX/TRAT
      NS=1
      RETURN
   10 CONTINUE
      NS=0
      RETURN
      END
```

TABLE A-7

Inputs

```
//G.SYSIN  DD  *,DCB=BLKSIZE=2000
 20450.25      1.0      3600.0
   5.0        2.76
   5.0       1.15        120.0
    3.0         60.0      0.27      0.040
   29.0         0.3       6.0        0.29      50000.0    50000.0    30000.0
   10.0         680.0     420.0
1               0.0
```

REFERENCES

1. Special summer program, 6.50S, Notes, M.I.T. 1972.

2. R. V. Harrowell, Preliminary Studies of Superconducting Alternators, Cryogenics, April 1972.

3. A.D. Appleton, Motors, Generators, and Flux Pumps, Cryogenics, June 1969.

4. L.M. Harvey and R.D. Fulmer, A New Concept of Electric Ship Propulsion, Marine Technology, April 1968.

5. P. Thullen, J.C. Dudley, D.L. Greene, J.L. Smith, Jr., H.H. Woodson, An Experimental Alternator with a Superconducting Rotating Field Winding, IEEE Transactions On Power Apparatus and Systems, Vol. PAS-90, No. 2, March/April, 1971.

6. H.H. Woodson, J.L. Smith, Jr., P. Thullen, and J.L. Kirtley, The Application of Superconductors in the Field Windings of Large Synchronous Machines, IEEE Transactions on Power Apparatus and Systems, Vol. PAS-90, No. 2, March/April 1971.

7. E.H. Sibley, E.G. Frankel, J.M. Reynolds, Superconductivity: Status and Implications for Marine Applications, SNAME, Symposium, 1966 Spring Meeting, Paper No. 8.

8. D.P. Greenisen, A Design Program for Superconducting Electrical Machines, MIT Thesis Nav. Eng., 1968.

9. D.L. Greene, Analysis of a Marine Propulsion System Incorporating Superconducting Electrical Machinery, MIT Thesis Nav. Eng., 1968.

10. E.F. McCann II, C.J. Mole, Superconducting Electric Propulsion Systems for Advanced Ship Concepts, Naval Engineers Journal, December 1972.

11. R.T. Miller, C.L.Long, S. Reitz, ASW Surface Ship of the "80's" Study, Naval Engineers Journal, December 1972.

12. T.A. Louie, General Electric Heavy-duty Gas Turbine Electric Propulsion for a Products Carrier, SNAME, Pacific Northwest Section, October 7, 1972.

13. General Electric, LM2500 Gas Turbine Electric Propulsion, Technical Description No. 90,503, January 1972.

14. General Electric, Heavy Duty Gas Turbine Electric Propulsion System for Phillips Petroleum LNG Tankers, Technical Description, TD-501, August 1972.

15. P. Mandel, A Comparative Evaluation of Novel Ship Types, SNAME Transactions, 1962.

16. J.L. Kirtley, Jr., Design and Construction of an Armature for an Alternator with a Superconducting Field Winding, MIT Thesis, Ph.D., August, 1971.

17. J.L. Kirtley, Jr., Basic Formulas for Air-core Synchronous Machines, MIT, Cambridge, Mass.

18. D.L. Luck, Electromechanical and Thermal Effects of Faults upon Superconducting Generators, MIT Thesis, Ph.D., June 1971.

19. S.P. Timoshenko, S. Woinowsky-Krieger, Theory of Plates and Shells, Second Ed., McGraw-Hill 1959.

20. G. Gerard, H. Becker, Handbook of Structural Stability, Part III-Buckling of Curved Plates and Shells, NACA TN-3783, August 1957.

21. Z.J.J. Stekly, State of the Art of Superconducting Magnets, Journal of Applied Physics, Vol. 42, No. 1, January 1971.

22. M.S. Lubell, State of the Art of Superconducting Magnets, Cryogenics, October 1972.

23. S.P. Timoshenko, Strength of Materials, D. Van Nostrand Company, 1950.

Thesis
D3524 Denizmen
Analysis of a super-
conducting generator
for ship propulsion.
145677